UNITED NATIONS UNIVERSITY
GEOTHERMAL TRAINING PROGRAMME
Orkustofnun, Grensásvegur 9,
IS-108 Reykjavík, Iceland

Reports 2009
Number 22

1-D JOINT INVERSION OF MT AND TEM DATA WITH EXAMPLES FROM THE KRÝSUVÍK AREA, REYKJANES PENINSULA, SW-ICELAND

Joseph Nyago
Department of Geological Survey and Mines
Ministry of Energy and Mineral Development
P.O. Box 9, Entebbe
UGANDA
jnyago@gmail.com

ABSTRACT

Electrical resistivity methods are widely applied in geothermal exploration. Any progressive work like exploration drilling in an area under study is always based on surface exploration results. In geophysical prospecting of geothermal systems, several geophysical exploration methods are applicable. This report focuses on the use of resistivity methods based on application of electromagnetic currents, such as Transient Electromagnetic (TEM) and Magnetotelluric (MT) methods, but other methods are also introduced and discussed briefly.

For tens of years, electromagnetic resistivity methods have turned out to be the most effective investigation tool in resolving anomalous subsurface resistivity structures associated with geothermal activity. In this report, a discussion of the fundamental principles and field practices involved in the different resistivity methods of interest are presented.

Existing TEM and MT resistivity data from Krýsuvík high-temperature geothermal area, SW-Iceland were interpreted and presented. Soundings were selected along a NW-SE profile through the area. The TEM data were inverted for 1-D, and a 1-D joint inversion of the MT and TEM data was also performed. A general interpretation of the results gives a plausible description of the resistivity structure of the study area.

1. INTRODUCTION

In the past few decades, application of geo-electrical methods in geothermal prospecting has proven to be a powerful tool. The use of electromagnetic (EM) resistivity methods has become increasingly more effective in characterizing and delineating potential geothermal reservoirs to an extent that even prospects with no surface manifestations have been resolved and delineated. Resistivity methods determine the variations in electrical resistivity of the subsurface both laterally and with depth. In this regard, methods such as Magnetotellurics (MT) and Transient Electromagnetics (TEM) based on the principles of naturally varying magnetic field and controlled magnetic field source techniques, respectively, have proven to be the most efficient methods in mapping the subsurface structure. TEM soundings probe to several hundred metres depth, but MT to tens or even hundreds of kilometres.

In this study, existing (10 TEM and 10 MT) soundings collected in Krýsuvík geothermal field were interpreted. The programs TEMX and SSMT2000 were used in the processing of the TEM and MT data, respectively. The TEMTD inversion program was used to perform Occam 1-D joint inversion of TEM and MT data so as to correct for static shift in MT soundings. Both TEMX and TEMTD were developed by Iceland GeoSurvey (ÍSOR) but SSMT2000 by Phoenix Geophysics, Canada. The results of the 1-D modelling were used to generate a resistivity cross-section perpendicular to the geological strike of the area.

Processing and interpretation of resistivity data presented in this report served as the main project work of the author, during his six months specialized training at the United Nations University Geothermal Training Programme (UNU-GTP). The resistivity data used is by courtesy of ÍSOR and the main objective of the study was to define the detailed resistivity structure beneath the unexploited Krýsuvík high-temperature geothermal area on the Reykjanes peninsula.

2. GEOPHYSICAL PROSPECTING IN GEOTHERMAL EXPLORATION

Almost all geophysical prospecting methods have been applied in geothermal exploration, but EM resistivity methods have proven to be more powerful in detecting and delineating exploitable reservoirs for both low- and high-temperature geothermal systems. In exploration of a geothermal reservoir, different geophysical prospecting methods are applied to measure the physical properties of the earth. The measurements are primarily done on the physical parameters that are sensitive to the temperature and fluid content of the rocks. The most important physical properties measured in geothermal exploration include electrical resistivity, temperature, magnetization, susceptibility, density, elasticity, seismic velocity, thermal conductivity and streaming potential. The results of the measurements are used to delineate the geothermal prospect, outline the drilling fields, locate aquifers and site production wells, and also estimate the properties of a given geothermal system. However, characterization of a geothermal system is based on fundamental parameters such as temperature, pressure, rock permeability/porosity and fluid salinity. A good geothermal reservoir has high temperature, high pressure, high porosity and permeability, and low content of dissolved solids and gases in the water.

2.1 Geophysical methods in geothermal exploration – a brief overview

Geophysical methods are applied in geothermal exploration based on the various parameters that are to be measured. These methods are classified as direct or indirect (Hersir and Björnsson, 1991). Direct methods are further categorized into thermal methods and electrical methods, whereas indirect (structural) methods include gravity, magnetic, and seismic methods.

Thermal methods are used for studying the thermal properties of geothermal systems by measuring the subsurface temperature. Measurements are made in shallow drill holes and in soil. Estimation of the temperature at depth can be obtained from the temperature gradient (Hersir and Björnsson, 1991). Therefore, thermal surveys can be used to delineate areas of enhanced thermal gradients, which is a basic requirement for geothermal systems.

Gravity methods can define density variations such as deep magmatic bodies that may signify the presence of the heat source. Gravity surveys are also very useful in geothermal areas under utilization to monitor the changes in groundwater level and mass balance in the system.

Magnetic methods are useful in mapping near-surface features such as tracing narrow linear dykes and faults, where the basement is covered with soil. Such structures are often of interest in geothermal

exploration, but the greatest potential for the method lies in its ability to detect the depth at which the Curie temperature is reached.

Seismic methods are divided into two subcategories: 1) Passive seismic methods deal with the detection and recording of natural seismicity and induced seismicity due to ground fracturing associated with geothermal fluid extraction and/or injection. The seismic activity gives information about active faults and therefore permeable zones in geothermal systems (Hersir and Björnsson, 1991). 2) Active seismic methods are concerned with seismicity generated by artificial wave sources. The propagation of the generated waves is used to study the geological structures and strata.

DC resistivity methods have been used for a long time in geothermal exploration with great success and the most common method is Schlumberger sounding. These methods can be applied both for depth sounding and profiling.

Electromagnetic methods are used to determine variations in the electrical resistivity of the earth with depth. The naturally varying field methods (MT) and controlled source methods (TEM), and a combination of these two methods have been adopted to better determine the variations in the electrical resistivity of the subsurface.

3. ROLE OF ELECTRICAL RESISTIVITY IN GEOTHERMAL PROSPECTING

3.1 Electrical resistivity of rocks

Resistivity methods have been found to be the most powerful methods in geothermal exploration (Árnason and Flóvenz, 1992; Eysteinsson et al., 1993). Besides direct surface manifestations, the resistivity of subsurface rocks is the most diagnostic parameter of geothermal activity that can be measured from the surface because the resistivity of rocks is strongly affected by the geothermal activity.

3.1.1 Factors affecting electrical resistivity of water-bearing rocks

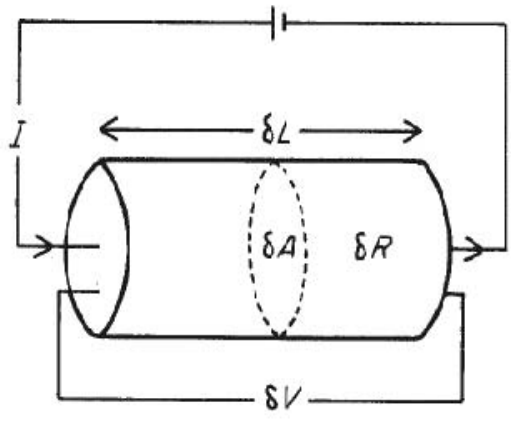

FIGURE 1: A conductive cylinder showing parameters used to define electrical resistivity (Kearey and Brooks, 1991)

Electrical resistivity of a material is a measure of its strength to oppose the flow of electric current through it. Electrical resistivity of rocks is a function of the rock type, porosity, permeability, alteration and fluids that fill the pore space. The resistivity of a water-bearing rock depends on the amount of water present, its salinity and also its distribution within the rock (Keller and Frischknecht, 1966). This implies that resistivity is directly related to the properties of interest such as salinity, temperature, alteration and porosity (permeability

The electrical resistivity of a conductive body is defined as the electrical resistance in Ohms (Ω) between the opposite faces of a unit cube of the conductive material. For a conducting cylinder (Figure 1), such as a rock material of resistance δR, length δL, and a cross-sectional area δA, its resistivity ρ is expressed by the equation:

$$\rho = \delta R \frac{\delta A}{\delta L} \tag{1}$$

where ρ = Resistivity (Ωm);
δR = Electrical resistance (Ω);
δA = Cross-section area (m^2);
δL = Length (m).

The reciprocal of resistivity is the conductivity given by:

$$\sigma = \frac{1}{\rho} \tag{2}$$

where σ = Conductivity (S/m).

According to Ohm's law, the resistivity of a material is defined mathematically as the ratio between electric field strength at a point in a material and the current density at that point, given by (Keller and Frischknecht, 1966):

$$\rho = \frac{E}{J} \tag{3}$$

where E = Electric field (V/m);
J = Current density (A/m^2).

The electrical conduction in most rocks is essentially electrolytic or due to secondary minerals. This is because most mineral grains are insulators. Thus the rock matrix itself is an insulator and the electric conduction occurs through an aqueous solution of common salts distributed throughout the pores of rocks and through alteration minerals at the rock-water interface. The electrical resistivity of rocks largely depends on the following rock properties:

- Rock porosity and permeability
- Salinity
- Temperature
- Pressure
- Fluid-rock interaction or alteration
- Saturation or amount of water

a) Rock porosity and permeability
Porosity φ of a material such as a rock is defined as the ratio of the pore volume to the total volume of a rock, given by the formula:

$$\varphi = \frac{V_\varphi}{V} \tag{4}$$

where φ = Fractional porosity;
V_φ = Volume of voids (m^3);
V = Total volume of the material (m^3).

Fluids are often important for electrical conduction of rocks. The degree of saturation and the porosity is of great importance to the bulk resistivity of the rock. The following empirical equations, usually referred to as Archie's law, describe how resistivity depends on porosity if ionic conduction dominates other conduction mechanisms in a rock (Archie, 1942; Hersir and Björnsson, 1991). Equation 5 is valid if the resistivity of the pore fluid is ≤ 2 Ωm:

$$\rho = \rho_w a \varphi_t^{-n} = \rho_w F \tag{5}$$

where ρ = Bulk resistivity (Ωm);
ρ_w = Resistivity of the pore fluid (Ωm);
φ_t = Porosity;
α = Empirical parameter describing the type of porosity varying from less than 1 for inter-granular porosity, to more than 1 for joint porosity, but is usually around 1;
n = Cementation factor, usually ≈ 2;
F = Formation factor, $F = a\varphi_t^{-n}$.

The permeability of a rock is the ability of fluids to flow within its matrix, and it is largely dependent on the size and shape of the pores in the substance. In granular materials such as sedimentary rocks, permeability depends on the size, shape, and packing of the grains. The amount of fluid flowing through a rock can also largely be dictated by fractures which are, as a result of secondary porosity, common in geothermal areas. The wider the fracture, the higher is the fracture porosity; hence, high permeability is expressed by:

$$\kappa = \frac{Q\eta L}{AP} \tag{6}$$

where κ = Permeability (m^2);
Q = Fluid flow rate (m^3/s);
η = Fluid viscosity (kg/ms);
L = Length of the rock (m);
A = Cross-sectional area available for flow (m^2);
P = Pressure drop (Pa).

Due to negligible electrical conduction in most minerals, charge mobility in rocks and sediments occurs in the electrolytes. High mobility of the charge carrier within a rock matrix due to high permeability has an effect of lowering the electrical resistivity of the rock. Geological processes such as faulting, shearing, columnar jointing and weathering increase permeability and porosity, resulting in an increase in electrical conductivity.

b) Salinity

An increase in the amount of dissolved ions in the pore fluid causes increasing conductivity as shown in Figure 2. The conductivity of a solution, σ, depends on the mobility and concentration (salinity) of the ions present in the solution, according to the following equation (Keller and Frischknecht, 1966):

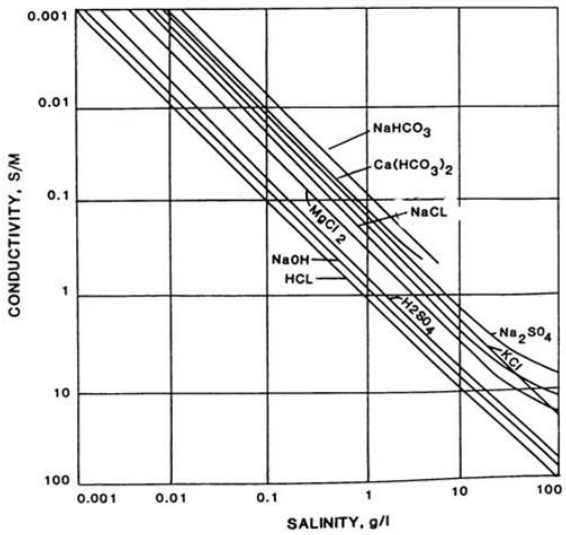

FIGURE 2: Pore fluid conductivity vs. salinity (concentration) for various electrolytes (modified from Keller and Frischknecht, 1966)

$$\sigma = \frac{1}{\rho} = F(c_1 q_1 m_1 + c_2 q_2 m_2 + ...) \tag{7}$$

where F = Faraday's number (*96,500 Coulombs);*
c_i = Concentration of ions;
q_i = Valence of ions;
m_i = Mobility of different ions.

An increase in both the water content and the total amount of dissolved ions is sometimes directly associated with geothermal activity.

c) Temperature
Dakhnov (1962) studied the relationship between the resistivity and temperature of rocks saturated with an electrolyte. At temperatures below 200°C, a rise in the temperature of an electrolyte decreases the viscosity, leading to an increase in the mobility of ions and, thus, lowering the resistivity. At higher temperatures, the dielectric permittivity of water reduces considerably, resulting in a decrease in the number of dissociated ions in the solution. This is illustrated by Figure 3 (Keller and Frischknecht, 1966). For temperatures lower than 200°C the variation of resistivity with temperature is approximately given by:

$$\rho_w = \frac{\rho_{w0}}{1+\alpha(T-T_0)} \tag{8}$$

where ρ_w = Fluid resistivity at temp., T;
ρ_{wo} = Fluid resistivity at temp., T_0;
α = Temperature coefficient of resistivity, 0.023 for T_0=23°C.

d) Pressure
Confining pressure has the net effect of increasing the bulk resistivity of a rock by decreasing pore volume as the rock is compressed. The pressure effect can be dramatic in fractured rock where the fractures normal to the principle stress close while others remain open. This leads to a significant change and anisotropy of the rock (Morris and Becker, 2001).

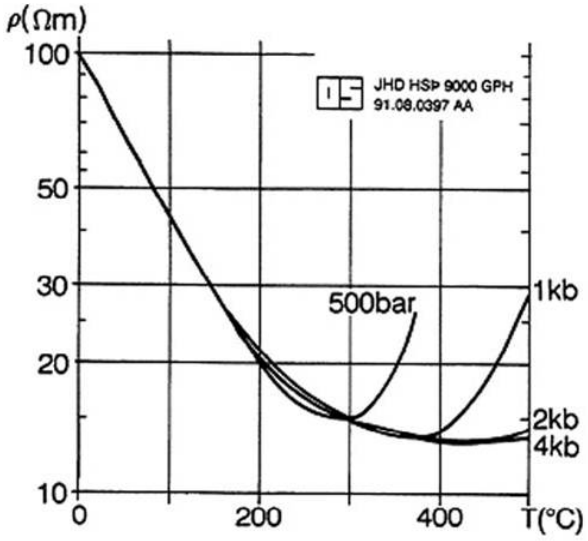

FIGURE 3: Resistivity of an electrolyte as a function of temperature at different pressures (modified from Hersir and Björnsson, 1991)

e) Fluid-rock interaction
Besides reduction in resistivity by the pore fluid, the bulk resistivity of the rock is also reduced by the presence of hydrous secondary minerals such as clays as a result of fluid-rock interaction. This interface conductivity (alteration) is expressed by the equation (Rink and Schopper, 1976):

$$\sigma = \left(\frac{1}{F}\right)\sigma_f + \sigma_s \tag{9}$$

where σ = Bulk conductivity (S/m);
σ_f = Conductivity of water (S/m);
σ_s = Interface conductivity (S/m);
F = Formation factor of the rock.

The interface conductivity is due to fluid-matrix interaction and depends mostly on rock type, temperature, fluid composition, the size of the internal surfaces (porosity) and on their nature.

In high-temperature geothermal systems (with temperatures higher than 200°C in the uppermost 1 km), there are widespread resistivity anomalies characterised by a low-resistivity cap at the outer

margins underlain by higher resistivity in the core of the system. There are two main reasons why the geothermal activity lowers the resistivity.

Firstly, the geothermal fluid has a higher concentration of dissolved ions (higher salinity) than cold groundwater and is therefore more conductive. Secondly, the thermal water interacts with the host rocks, forming secondary alteration minerals. Some of these minerals, such as clay minerals (smectite) and zeolites are conductive and reduce the resistivity of the rock formation. The alteration process and the resulting type of alteration minerals are dependent on the type of primary minerals, and the chemical composition and temperature of the geothermal fluid. Furthermore, the intensity of the alteration is dependent on the temperature, time and texture of the host rock. At relatively low temperatures, or below 200°C, the alteration minerals are mainly conductive. On the other hand, at higher temperatures, the minerals are predominantly resistive. The temperature where the transition from conductive to resistive minerals occurs depends on the rock type. In acidic rocks it occurs in the range of 180-200°C, but in basic rocks it happens within the range of 220-240°C as shown in Figure 4 (Árnason et al., 2000, Flóvenz et al. 2005).

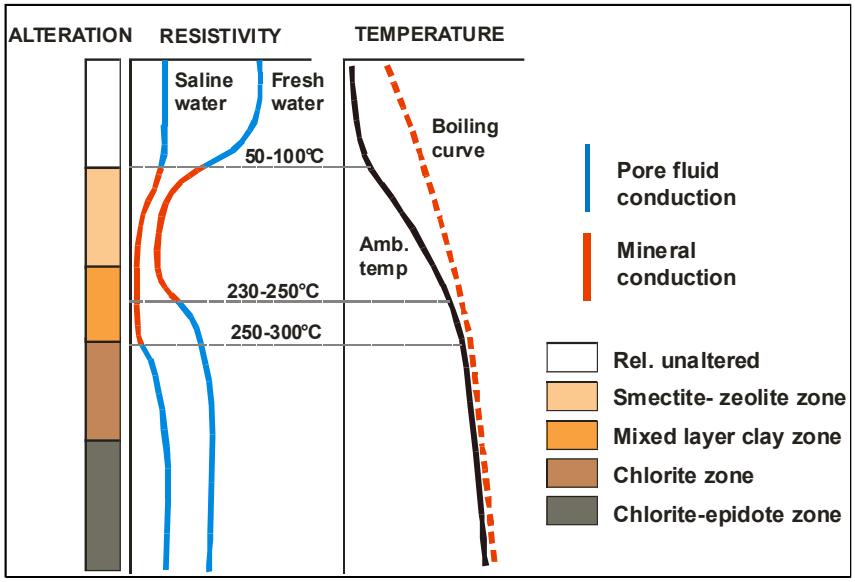

FIGURE 4: A summary of general resistivity structures of basaltic crust beneath Iceland (modified from Flóvenz et al., 2005)

3.2 Electrical methods

Application of electrical methods can either be as sounding or profiling (Hersir and Björnsson, 1991). A sounding is used to map resistivity variation with depth while profiling is used for mapping lateral resistivity variations at an approximately constant depth. The electrical methods are also classified into direct current methods and electromagnetic methods.

Direct current (DC) methods: A time independent current distribution is created in the subsurface by injecting a constant current into the earth through a pair of electrodes placed on the surface. The current induces a potential field in the earth. The potential difference is measured over a short distance; hence, the information on the subsurface resistivity can be obtained. Depending on the type of electrode arrangement applied, DC methods are categorized as Schlumberger sounding, head-on resistivity profiling, dipole-dipole profiling and sounding, etc. Soundings are resistivity measurements as a function of depth, using different distances between current electrodes, where as profiling measures lateral changes in resistivity at nearly constant depth with measurements taken at fixed intervals between current electrodes placed at different points on the surface (Tugume, 1995).

Electromagnetic (EM) methods: EM methods are also referred to as alternating current (AC) methods because they make use of alternating current induced in the earth. It may be artificially induced or naturally induced signals. Therefore, EM methods are also subcategorized into natural source electromagnetic methods and controlled source electromagnetic methods.

In natural source methods such as magnetotelluric (MT) and audio-magnetotelluric (AMT), fluctuations in the natural magnetic field of the earth induce an electrical field. By measuring these fields, information on the resistivity structure can be obtained.

In controlled source methods such as the time domain or transient electromagnetic (TEM) method, a magnetic field is generated by transmitting a constant current of known magnitude through a loop or grounded dipole. When the current is abruptly turned off the magnetic field starts to decay with time. This is used to determine the resistivity structure.

4. APPLICATION OF ELECTROMAGNETIC RESISTIVITY METHODS

Electromagnetic resistivity methods measure the electrical conductivity of the subsurface at relatively low frequencies. EM methods have proven their efficiency in investigating the depth to good conductors; their applications have largely phased out the use of the conventional DC resistivity methods such as Schlumberger soundings, and they are found to be more cost-effective for prospecting. The MT sounding method is capable of probing to depths of several tens to even hundreds of kilometres, while the central-loop TEM sounding method is sort of downwardly focused to what is vertically below the source loop and probes to 0.5 -1 km depth.

In time domain electromagnetics such as TEM, current is induced in the ground by a time-varying magnetic field of known strength generated by a source loop or a grounded dipole, and the monitored signal is the decaying magnetic field at the surface. The current transmitter couples inductively to the earth, and no current has to be injected into the ground as in the case of DC soundings (Árnason, 1989).

MT is effective because of its wide depth range due to the varying frequencies of the earth´s natural, time-variable electromagnetic field. The ability of the MT sounding method to detect deep conductors embedded in resistive media is related to the dimensions of the conductor, the resistivity contrast between the conductor and the host rocks, and also the specific electro-stratigraphic distribution of the area under investigation (Volpi et al., 2003).

4.1 The central-loop TEM method

4.1.1 Basic principles

In the central-loop TEM sounding method, the earth is excited using a transmitter. A loop of wire is laid on the ground and a constant current is transmitted through the loop to build up a constant magnetic field of known strength. When the current is turned off in a controlled manner by the transmitter, the magnetic field starts to decay and, at the same time, induces secondary electrical currents in the ground which, in turn, induce a secondary magnetic field also decaying with time. The decay rate of the secondary magnetic field is then monitored by measuring the voltage induced in a receiver coil or a small receiver loop at the centre of the current transmitting loop. The distribution of the current (Figure 5) and the rate of decay of the secondary magnetic field both depend on the resistivity structure of the earth.

At later times are affected by conductivity at greater depths than the depths of those which affected the earlier signals. Therefore, the rate of decay recorded as a function of time after the current in the transmitting loop is switched off, can be interpreted in terms of the subsurface resistivity structure (Árnason, 1989).

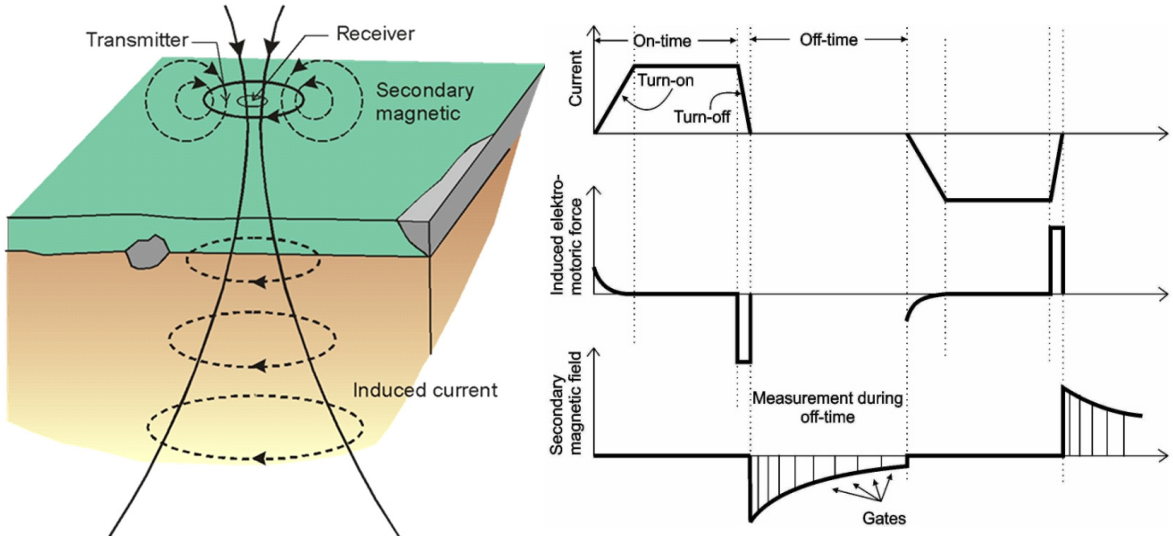

FIGURE 5: Central loop TEM configuration and plots showing the transmitted current and the magnetic field response (taken from Árnason, 2006; and Kurt et al., 2006)

The voltage induced in the receiver coil at the centre of a circular source loop of radial r with harmonic current $I = I_0 e^{i\omega t}$ on the surface of a layered earth (Figure 6) is given by (Árnason, 1989):

$$V(\omega, r) = A_r n_r A_s n_s I_0 e^{i\omega t} \frac{-i\omega\mu_0}{\pi r} \int_0^\infty \frac{\lambda^2}{m_0} \frac{S_0}{S_0 - T_0} J_1(\lambda r)\, d\lambda \tag{10}$$

where A_r = Cross-sectional area of the receiver coil (m^2);
A_s = Cross-sectional area of the transmitter loop (m^2);
n_r = Number of windings in the receiver coil;
n_s = Number of windings in the transmitter loop;
I_0 = Transmitter current (A);
μ_0 = Magnetic permeability in vacuum (H/m);
r = Radius of the transmitter loop (m);
J_1 = Bessel function, first kind, order 1.

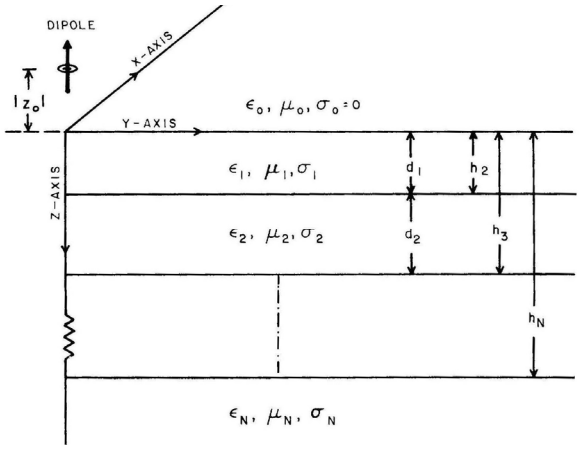

FIGURE 6: The N-layered earth (taken from Árnason, 1989)

S_0 and T_0 contain the parameters of the layered earth, and are determined by the recurrence relationship:

$$S_{i-1} = S_i \cosh(m_i d_i) - T_i \sinh(m_i d_i) \tag{11}$$

$$T_{i-1} = -\frac{m_i}{m_{i-1}} [S_i \sinh(m_i d_i) - T_i \cosh(m_i d_i)] \tag{12}$$

with

$$S_{N-1} = 1$$

and

$$T_{N-1} = -\frac{m_N}{m_{N-1}}$$

where d_i = Thickness of the i^{th} layer (m);
m_i = Impedance of the i^{th} layer (m^{-1}).

The quantities,S_0 and T_0 in Equations 11 and 12, depend on angular frequency (ω) and conductivity (σ), through $m_i = \sqrt{\lambda^2 - k_i^2}$ where $k_i^2 = \omega^2\mu_i\varepsilon_i - i\omega\mu_i\sigma_i$ where σ_i is the conductivity of the i^{th} layer (i=0, 1, ... ,N) and ε is the dielectric permittivity. Due to the small value of ε (normally smaller than 10^{-10}), k can be approximated, for low frequencies, in the quasi-stationary approximation, as $k_i^2 = -i\omega\mu\sigma$.

The mutual impedance between the source and the receiver coil, given by Ohm's law analogy is defined by the ratio between the measured voltage and the transmitted current. From Equation 10, the mutual impedance is then given by:

$$Z(\omega, r) = \frac{V(\omega, r)}{I_0 e^{i\omega t}} = A_r n_r A_s n_s \frac{-i\omega\mu_0}{\pi r} \int_0^\infty \frac{\lambda^2}{m_0} \frac{S_0}{S_0 - T_0} J_1(\lambda r)\, d\lambda \tag{13}$$

Equation 13 can be transformed into a time domain by Fourier expansion of the function describing the transmitted current. By describing the transmitted current as a function *I(t)*, a Fourier expansion of the current function can be given by (Árnason, 1989):

$$I(t) = \frac{1}{(2\pi)^{1/2}} \int_{-\infty}^{\infty} \tilde{I}(\omega) e^{i\omega t}\, d\omega \tag{14}$$

If a constant current I_0 is turned off at t = 0, $\tilde{I}(\omega) = -\frac{I_0}{i\omega}$. The measured voltage, as a function of time after the steady current is abruptly turned off at t = 0 is then expressed as:

$$V_-(t) = \frac{-I_0}{2\pi} \int_{-\infty}^{\infty} \frac{Z(\omega)}{i\omega} e^{i\omega t}\, d\omega = \frac{I_0}{2\pi} \int_{-\infty}^{\infty} \phi(\omega) e^{i\omega t}\, d\omega \tag{15}$$

In the case where I_0 is turned on at t = 0, $\tilde{I}_+(\omega) = -\tilde{I}_-(\omega)$ and $V_+(t) = -V_-(t)$. For simplicity, we define:

$$\phi(\omega) = \frac{Z(\omega)}{-i\omega} \tag{16}$$

$\phi(\omega)$ only depends on ω through ω^2 and $i\,\omega$, hence:

$$\phi^*(-\omega) = \phi(\omega) \tag{17}$$

where * denotes a complex conjugate.

Therefore:

$$\mathrm{Re}\,\phi(-\omega) = \mathrm{Re}\,\phi(\omega) \quad \text{and} \quad \mathrm{Im}\,\phi(-\omega) = -\mathrm{Im}\,\phi(\omega) \tag{18}$$

Equation 17 can then be simplified to:

$$V\_(t) = \frac{2I_0}{\pi}\int_0^{\infty} \mathrm{Re}\,\phi(\omega)\cos(\omega t)\,d\omega$$

or

$$V\_(t) = \frac{-2I_0}{\pi}\int_0^{\infty} \mathrm{Im}\,\phi(\omega)\sin(\omega t)\,d\omega \qquad (19)$$

In practice, the current is not abruptly turned off, but it is turned off linearly in a time interval of length *TOFF*. Transient voltage generated in the receiver coil due to a linearly ramped step function is given by (Árnason, 1989):

$$V(t) = \frac{1}{TOFF}\int_{-TOFF}^{0} V\_(t-\tau)\,d\tau = \frac{1}{TOFF}\int_{t}^{t+TOFF} V\_(\tau)\,d\tau \qquad (20)$$

For a homogeneous half-space of conductivity σ, the induced voltage in the receiver coil at late time after current turn-off, can be worked out analytically, and is given by (Árnason 1989):

$$V(r,t) \approx I_0 \frac{C(\mu_0\sigma r^2)^{3/2}}{10\pi^{1/2}t^{5/2}} \qquad (21)$$

where $C = A_r n_r A_s n_s \frac{\mu_0}{2\pi r^3}$

The above can be solved to obtain the resistivity of the half-space. The formula can then be used to define the late-time apparent resistivity (Árnason 1989):

$$\rho_a = \frac{\mu_0}{4\pi}\left[\frac{2I_0\mu_0 A_r n_r A_s n_s}{5t^{5/2}V(r,t)}\right]^{2/3} \qquad (22)$$

where t = Time elapsed after the transmitter current is turned to zero (s);
A_r = Cross-sectional area of the receiver coil (m^2);
n_r = Number of windings in the receiver coil;
A_s = Cross-sectional area of the transmitter loop (m^2);
n_s = Number of windings in the transmitter loop;
μ_0 = Magnetic permeability in vacuum (H/m);
I_0 = Transmitter current (A);
$V(r,t)$ = Measured voltage (V).

4.1.2 The TEM field measurements

Instrumentation and configuration: In order to become more acquainted with the operation of the TEM instruments and data acquisition procedures, a single day of fieldwork was used in the Krýsuvik area. The time domain electromagnetic PROTEM-67 instruments manufactured by Geonics Ltd, Canada, were used. They consist of a digital receiver with a built-in data logger, a receiver coil (effective area 100 m^2) and a square receiver loop (effective area 5613 m^2), a motor generator, current transmitter coupled to external power module and current transmitting loop (wires). The field work was carried out under the supervision of the ÍSOR geophysical staff.

The digital receiver monitors the transient decay of the secondary magnetic field by measuring the voltage induced in the receiver coil centrally positioned in the current transmitting loop. The digital receiver and current transmitter timings are controlled by synchronized precision crystal clocks. The voltage induced in the receiver coil is always measured by the receiver each time the transmitted

current is turned off. The TEM instrument transmitted half duty square wave current and can be operated at different frequencies, 0.25, 2.5 and 25 Hz.

Field procedure: During the set up of the TEM sounding, a 300 m by 300 m square transmitter loop was laid out and a half duty square wave current of approx. 22 A was transmitted into the loop. In order to get rid of both external and internal noise in the data, the induced voltage measured was stacked over many cycles. Due to the induced voltage decreasing rapidly with time, the low-frequency signals were measured both with the standard circular receiver coil (100 m^2) and with a flexible loop of relatively large area (5613 m^2) to obtain a stronger output signal.

The data were automatically stored in the memory of the data logger together with the corresponding configurations (settings) such as station code, transmitted current, frequencies, current loop area, gains and turn-off time.

4.2 The magnetotelluric (MT) method

4.2.1 Basic principles and Maxwell's equations

The magnetotelluric (MT) method is a passive frequency-domain electromagnetic sounding technique that measures the earth´s response to natural electric (telluric) and magnetic fields to investigate the resistivity structure of the subsurface. The MT method exploits naturally varying EM fields, spanning from 0.0001 Hz to 10 kHz. These primary fields induce secondary electric and magnetic fields in the conductive earth. The EM fields recorded at the surface of the earth are, therefore, diagnostic to the electrical properties. Telluric currents are caused to flow in the earth by the earth's varying magnetic field. The EM waves of the MT signals are mainly caused by distant lightning (above 1 Hz), and electric currents flowing in the ionosphere (below 1 Hz). The EM field caused by these changing currents radiates around the earth, reflected repeatedly between the conductive ionosphere and the relatively conductive earth (Vozoff, 1990).

The popularity of the MT sounding method in geothermal prospecting has increased through the years due to its great depth of investigation and effectiveness in delineating high conductivity zones associated with high temperature (Zhdanov and Keller, 1994). The method has been widely applied in deep prospecting of high-temperature geothermal fields in Iceland (e.g. Árnason et al., 2009).

Modern surveys are conducted by measuring two perpendicular horizontal, x and y components of the electric and magnetic fields ($\boldsymbol{E}$ and $\boldsymbol{H}$), and the vertical, z component of $\boldsymbol{H}$ as a function of time. The time series recorded are then Fourier transformed to the frequency domain for further processing, determining the impedance tensor, apparent resistivities and phases (see later).

The behaviour of electromagnetic fields (EM) is concisely described by Maxwell's equations that define the fundamental relationship between the electromagnetic field vectors. The equations are based on Faraday´s and Ampere´s laws, and are given by:

$$\boldsymbol{\nabla} \times \boldsymbol{E} = -\frac{\partial \boldsymbol{B}}{\partial t} \tag{23}$$

$$\boldsymbol{\nabla} \times \boldsymbol{B} = \boldsymbol{J} + \varepsilon \frac{\partial \boldsymbol{E}}{\partial t} \tag{24}$$

Another important relationship in EM studies is a constitutive equation, derived from Ohm´s Law. The most common form of this law is $V = IR$. In terms of current density, $\boldsymbol{J}$, the law can be expressed as:

$$\boldsymbol{J} = \sigma \boldsymbol{E} \tag{25}$$

where σ = Conductivity (S/m); and
$\boldsymbol{E}$ = Electric field strength (V/m).

As an electromagnetic wave propagates through the earth, its amplitude decays exponentially with depth at a rate dependent on the conductivity of the medium and the frequency of the wave. Longer periods (low frequencies) decay more slowly with depth and therefore penetrate deeper. Hence, information about the near-surface and deep structure is deduced from high-frequency and low-frequency variations, respectively.

In a homogeneous half space with uniform resistivity, ρ, the depth at which the amplitude of the electromagnetic wave (Figure 7) reduces to e^{-1} (about one third) of its amplitude at the surface is known as the skin depth, δ, which is an approximate measure for the depth of penetration given (in km) by:

$$\delta \approx 0.5(\rho T)^{1/2} \tag{26}$$

where ρ = Resistivity (Ωm);
T = Period of the EM wave (s).

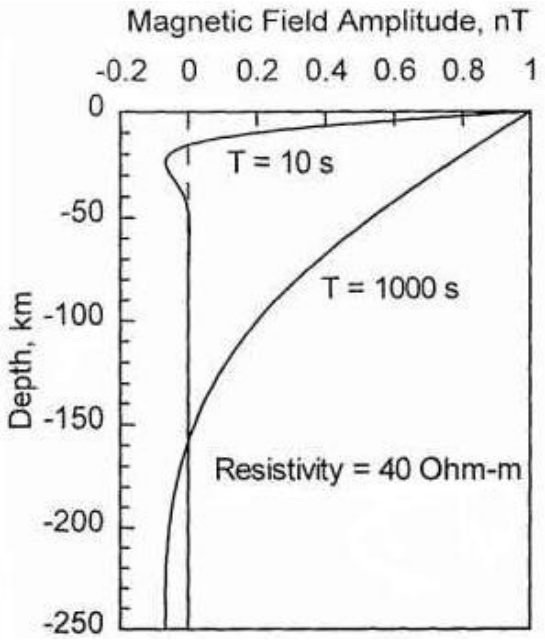

FIGURE 7: The decay of amplitude of the magnetic field signal for two periods in a homogeneous earth (Hermance, 1995)

The fluctuating magnetic (source) field, ***H,*** propagates vertically downwards below the earth's surface inducing an electric field, ***E***, in the subsurface. Their relationship at each frequency involves a characteristic impedance tensor, *Z,* given by (Hermance, 1973):

$$\begin{bmatrix} E_x \\ E_y \end{bmatrix} = \begin{bmatrix} Z_{xx} & Z_{yx} \\ Z_{xy} & Z_{yy} \end{bmatrix} \begin{bmatrix} H_x \\ H_y \end{bmatrix} \quad \text{or} \quad \vec{E} = \left[\overline{\overline{Z}}\right]\vec{H} \tag{27}$$

Therefore, in a Cartesian coordinate system at the earth's surface, with the ***E*** and ***H*** fields having *x*-north, *y*-east and *z*-vertical downward components, Equation 27 is rewritten as:

$$\begin{aligned} E_x &= Z_{xx}H_x + Z_{xy}H_y \\ E_y &= Z_{yx}H_x + Z_{yy}H_y \end{aligned} \tag{28}$$

where, Z_{xy}, and Z_{yx} are the principal impedances and Z_{xx}, Z_{yy} are the supplementary ones, contributed from parallel components of the electric and magnetic fields.

For a homogeneous or layered (1-D) earth, *Z* simplifies such that $Z_{xx} = Z_{yy} = 0$ and $Z_{yx} = -Z_{xy}$. The characteristic impedance, *Z* is then given by (Vozoff, 1990):

$$Z = \begin{bmatrix} 0 & Z_{xy} \\ -Z_{xy} & 0 \end{bmatrix} \tag{29}$$

In a 2-D case, if one of the coordinate directions is along the strike, the *Z* matrix is given as:

$$Z = \begin{bmatrix} 0 & Z_{xy} \\ Z_{yx} & 0 \end{bmatrix} \tag{30}$$

From the classical theory of EM wave propagation in a linear homogeneous isotropic and conductive medium, a plane wave propagates such that the electric field, ***E*** and the magnetic field, ***H*** are orthogonal to each other and orthogonal to the direction of propagation., The crosspower, ***E*×*H***, is the power flow along the direction of propagation (Hermance, 1995).

In this case, the ratio of the electric field component to the magnetic field intensity in an orthogonal direction is a characteristic measure of the EM properties of the medium referred to as the characteristic impedance, *Z*, given by:

$$Z = \frac{E_x}{H_y} = -\frac{E_y}{H_x} = \frac{i\omega\mu_o}{k} \tag{31}$$

where Z = Characteristic impedance (Ω);
E_x , E_y = Electric field components in x, y direction (V/m);
H_x, H_y = Magnetic field components in x, y direction (A/m);
ω = Angular frequency ($2\pi f$);
f = Frequency (Hz);
k = Wave number.

For a homegeneous halfspace and by neglecting the displacement currents ($\varepsilon \approx 0$), the impedance can be rewritten as:

$$Z = \frac{\omega\mu}{\sqrt{-i\omega\mu\sigma}} = \sqrt{i}\sqrt{\omega\mu\rho} = (\omega\mu\rho)^{1/2} e^{i\pi/4} \tag{32}$$

where *Z* is a complex number made of both real and imaginary parts or amplitude and phase..

For a homogeneous earth, the resistivity is given by the following equation, while the phase difference between E_x and H_y is 45° with H_y lagging E_x by π/4 (Figure 8):

$$\rho = \frac{1}{\omega\mu}|Z|^2 = 0.2T\left|\frac{E_x}{H_y}\right|^2 \tag{33}$$

and

$$\theta = \arg(Z_0) = \pi/4 = 45^\circ$$

For a non-homogeneous earth, the apparent resistivity, ρ_a and phase are defined by:

$$\rho_a = \frac{1}{\omega\mu}|Z|^2 = 0.2T\left|\frac{E_x}{H_y}\right|^2 \quad ; \quad \theta = \arg(Z_0) \neq 45^\circ \tag{34}$$

and are now functions of frequency.

In a horizontally layered earth, the impedance of the electromagnetic plane wave is given by the recursive formula (Ward and Wannamaker, 1983):

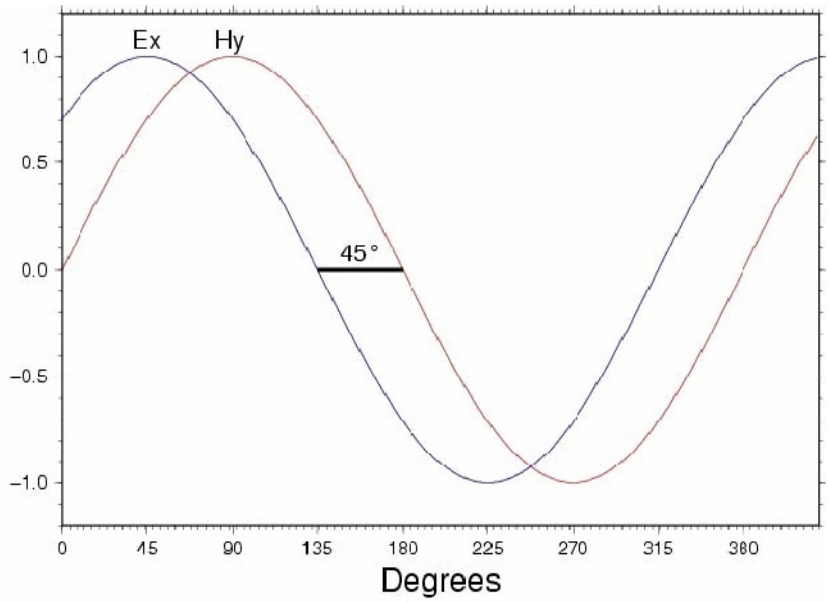

FIGURE 8: Phase difference of the *E* and *H* fields

$$\hat{Z}_{n-1} = Z_{n-1}\frac{\hat{Z}_{n-1}\tanh(ik_{n-1}h_{n-1})}{Z_{n-1}+\hat{Z}_n\tanh(ik_{n-1}h_{n-1})} \tag{35}$$

for which n = N-1,..1, and the term $Z_n = \mu_0\omega/k_n$ is the intrinsic impedance of the i^{th} layer, $\hat{Z}_i$ is the impedance at the top of the i^{th} layer, while k_i and h_i are the wave number and thickness of the i^{th} layer.

Equation 35 can then be used to derive the impedance, phase, θ and the apparent resistivity ρ_a, expressed as:

$$\hat{Z}_0 = \left|\hat{Z}_0\right|e^{i\theta}, \quad \rho_a = \frac{1}{\omega\mu_0}\left|\hat{Z}_0\right|^2 \quad \text{and} \quad \theta_a = \arg(Z_0) \tag{36}$$

4.2.2 The magnetotelluric field measurements

Instrumentation: Two days of field work were devoted to demonstrate the operation of the MT equipment. In this case, a five-channel MT data acquisition system (MTU-5A), a product of Phoenix Geophysics, Canada was used. A five component layout consists of the following hardware:

- MTU-A acquisition unit (data logger with a memory card);
- GPS antenna;
- 5 electrodes;
- 3 magnetic field induction coils;
- Connecting cables;
- 12 volt DC battery.

Field procedure: A typical layout of a five component MT unit (see Figure 9) consists of 5 electrodes, 4 of which measure 2-perpendicular horizontal components of the electric field (E_x,E_y), and the fifth electrode is used to ground the MTU data logger at the centre. For magnetic field measurement, 3 induction coils are involved, 2 of which measure 2-horizontal perpendicular components (H_x,H_y), and 1 coil measures the vertical component (H_z) of the magnetic field as shown in Figure 9.

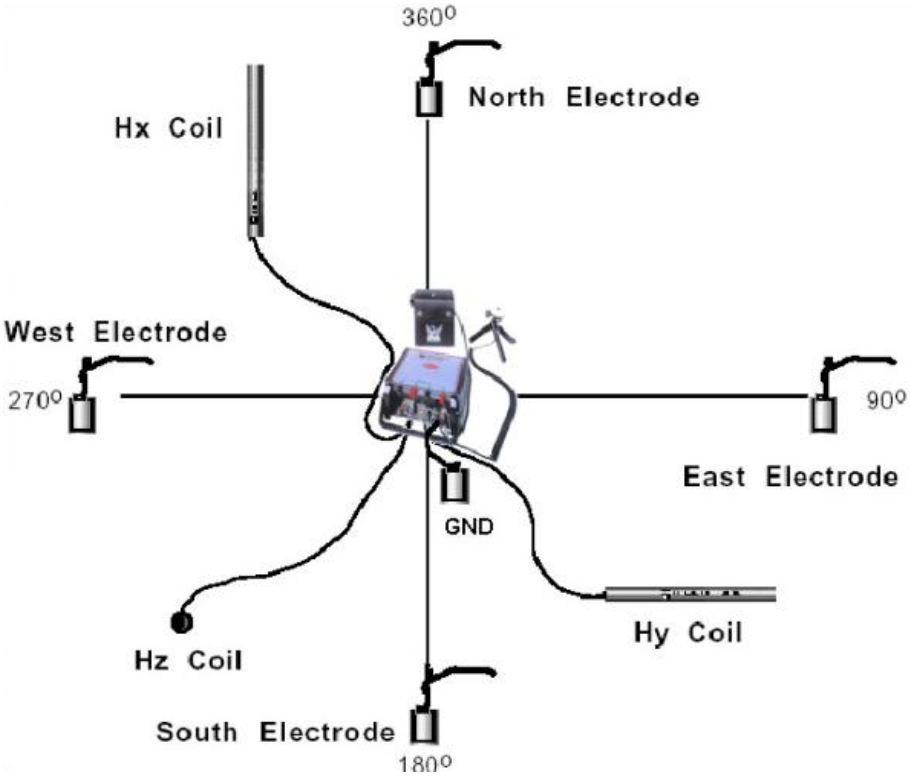

FIGURE 9: A field layout of a 5-channel MT site (modified from Phoenix Geophysics, 2003)

At each MT site, timing is obtained from the GPS time signals. A remote reference station is placed tens of kilometres away for noise reduction techniques. During the fieldwork in Krýsuvík area, two MT sounding sites were set up, comprising 2- (E_x and E_y), and 5-channels MTU units. To minimise wind noise, the coils and cables were buried in the ground, giving an additional advantage of reducing thermal effects on the induction coils. The instruments were left to run for 2 days. The equipment deployment was carried out under the supervision of ÍSOR geophysical staff.

Remote reference site: A remote reference technique involves measuring magnetic field variations simultaneously at two sites separated by a long distance. This technique allows removing signals that are not common in the two data sets. The procedure ensures that all inducing signals are associated with vertically travelling planar waves. The signals discarded are possibly noise caused by electrical noise in the equipment and cultural noise from nearby power lines, radio transmitters and electric fences.

4.2.3 Static shift effects and correction

The MT sounding method, like all resistivity methods that are based on measuring the electric field in the subsurface, suffers the so called telluric or static shift problem. The phenomenon is caused by shallow resistivity inhomogeneities close to the electric dipoles, and can cause severe problems in the interpretation of MT data by shifting the apparent resistivity sounding curves (on a log scale) by a scale factor, which is independent of frequency. The amount of parallel shift cannot be determined directly from conventionally recorded MT data at a single site (Sternberg et al., 1988).

One method to correct for static shift is to carry out central-loop TEM sounding at the same site. The TEM does not suffer the static shift problem because the decaying magnetic field at the surface is much less affected by local inhomogeneities than the electric field associated with MT. Telluric shift correction in the MT is achieved by jointly inverting the MT and TEM sounding data collected at the same location. This approach has since proved to be the most consistent solution.

5. KRÝSUVÍK HIGH-TEMPERATURE GEOTHERMAL AREA

5.1 Geology and tectonics of Krýsuvík

Krýsuvík is located on the Reykjanes Peninsula in SW-Iceland, about 25 km from the capital, Reykjavík. It is one of four high-temperature geothermal areas on the peninsula (Figure 10). The geothermal areas lie along the plate boundary, where the en-echelon arranged fault swarms cross the boundary at a strike angle of 40°. Krýsuvík itself is divided into five subfields, namely: Trölladyngja, Hveradalir-Seltún, Austurengjar, Köldunámur and Sandfell geothermal fields (Ármannsson et al., 1994).

Generally, the outer Reykjanes peninsula on which Krýsuvík field is situated is characterised by extensive postglacial lava fields, and steep-sided mountains and ridges of pillow lavas, pillow breccias, and hyaloclastites protruding through the lava fields. The hyaloclastites are of upper Quaternary age from the last glaciations, formed during volcanic eruptions within the ice. The hyaloclastite ridges are striking approximately N40ºE and originate from eruptive fissures. The hyaloclastite ridge of Sveifluháls is believed to have been formed during the last glaciation (Imsland, 1973; Jónsson, 1978). The ridge is composed of four eruptive formations and was possibly built up during four volcanic episodes (Imsland, 1973). The rocks in the area are entirely of basaltic composition, with lava fields dominating most of the west low-lying part of the Reykjanes Peninsula. The postglacial volcanic activity that has occurred on the peninsula consists of fissure eruptions and central eruptions, where the latter resulted in rather flat cones.

The central eruptions are more common than the fissure eruptions. It is likely that during the prolonged eruptions the activity tended to be strongly concentrated in a single vent although the magma may initially have forced its way through the fissures.

5.3 Previous geophysical studies

Resistivity surveys based on Schlumberger configuration were conducted in Krýsuvík area to estimate the resistivity of the bedrock at different depths (Arnórsson et al., 1975). About 70 DC electrical depth soundings were made, and the current arm varied between 0.9 and 1.5 km. Due to the rugged

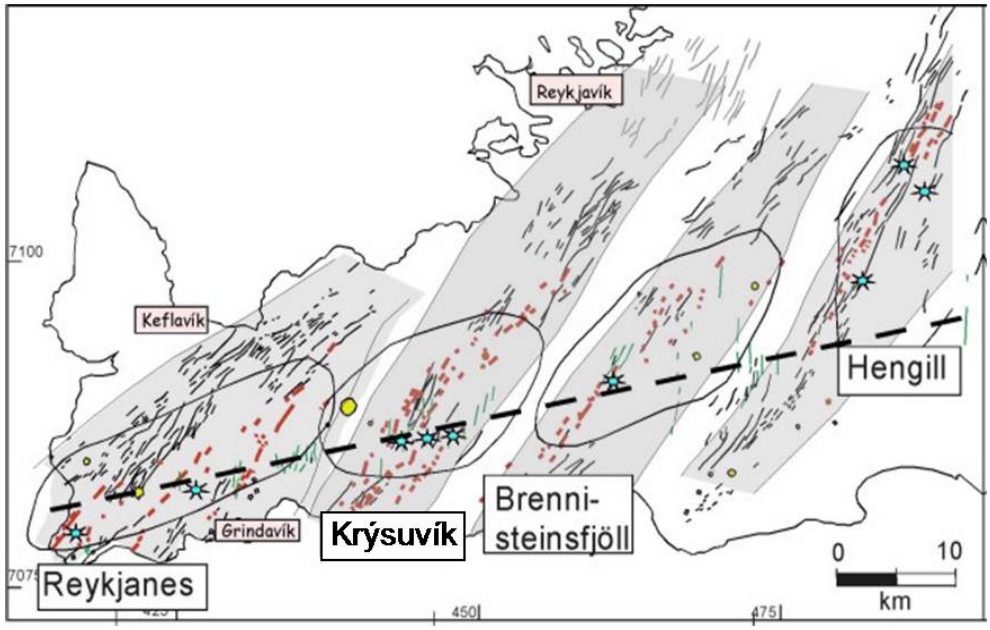

FIGURE 10: Tectonic map of the outer Reykjanes peninsula showing fissure swarms and geothermal fields (Clifton, 2007)

terrain of the area, the resistivity map is somewhat incomplete; only a few soundings were made on the hyaloclastite ridges. However, dipole-dipole measurements with a 1.5 km dipole spaced along the Sveifluháls indicated resistivity values in the range of 5-8 Ωm under the ridges at an approximate depth of 1 km. Additional soundings were done in the late seventies and early eighties giving a different and more complete picture of the area, showing several upflow zones (Flóvenz et al., 1986).

Magnetotelluric measurements revealed the resistivity at 10 km depth. A magnetotelluric station was deployed between the two hyaloclastite ridges and recorded both magnetic and electrical fields. Estimates for the apparent resistivity were computed and the shallower depths of the MT results were fitted with the Schlumberger and dipole-dipole soundings. The top of the deep high-resistivity layer coincides with the upper boundary of a seismic layer with a P-wave velocity close to 6.5 km/sec (Pálmason, 1971). An airborne magnetic survey that was flown in the area did not reveal any magnetic lows over the hydrothermal area.

6. PROCESSING AND 1-D INVERSION OF RESISTIVITY DATA

In this study, 10 TEM and 10 MT soundings in Krýsuvík area were processed and interpreted. Figure 11 shows the location map of the soundings. They were collected along profile KRY9 during the previous surveys conducted in 2007, 2008 and early 2009 (Hersir et al., 2009). The TEM raw data files and MT time series were first processed. Then the TEM and MT data were converted into standard input format ready for application of an interpretation program. The rotationally invariant

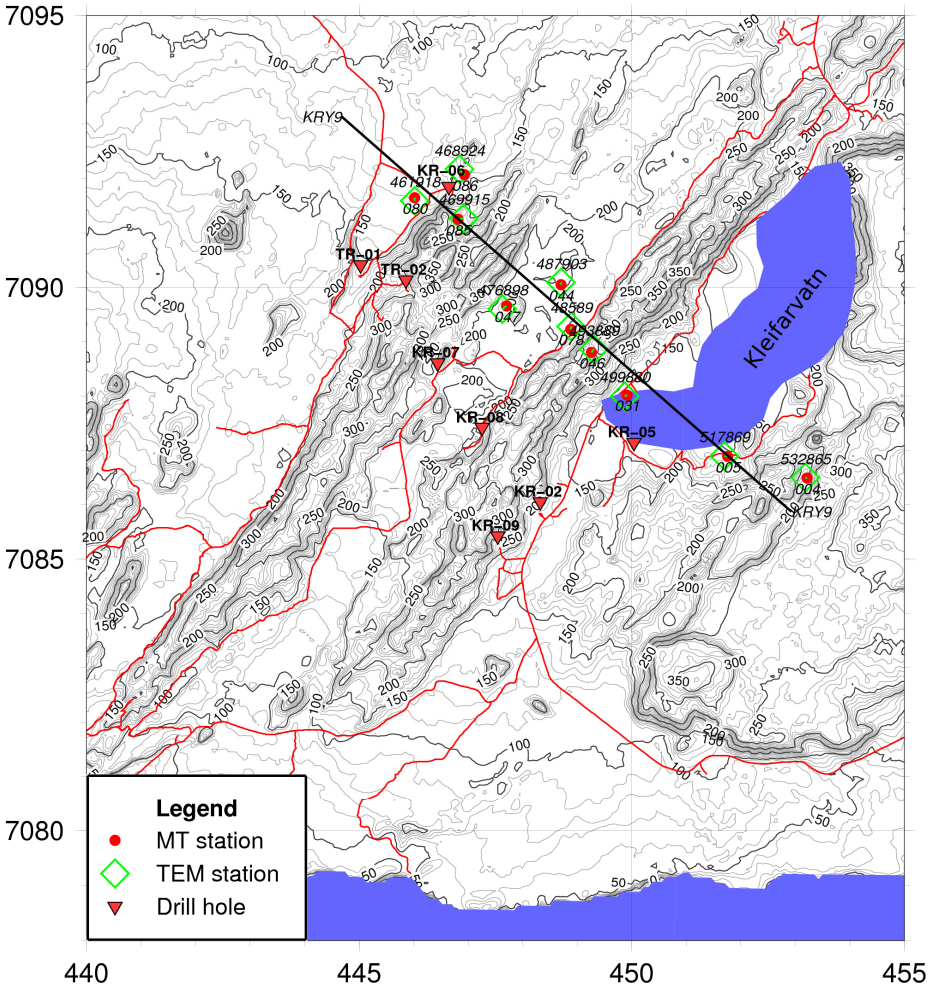

FIGURE 11: Location map of MT and TEM soundings and drill holes in the Krýsuvík area

apparent resistivity and phases derived from the determinant of the MT tensor were inverted jointly with the TEM data by 1-D inversion. This gives layered models from shallow to great depths and determines the best static shift parameter for the MT data. Static shift values obtained fell in a range between 0.3 and 1.5.

6.1 Processing and interpretation of TEM data

TEM data processing was done using TEMX, a program developed by ÍSOR geophysical staff. The program reads raw data files in a format directly downloaded from the PROTEM receiver. The program calculates the averages and standard deviations of the repeated transient voltage measurements and computes late time apparent resistivity as a function of time. The program runs under a UNIX/LINUX environment. The program also offers an option in graphical interface for rejecting noisy data. At this stage an interpretation program, TEMTD, also developed by ÍSOR is used to perform a separate 1-D layered-earth inversion on the TEM data (Árnason, 2006), see Appendix I.

With TEM soundings, TEMTD assumes that the source loop is square and that the receiver coil or loop is positioned right at the centre of the current source loop. The current wave form is assumed to be a half-duty bipolar semi-square wave with exponential current turn-on and linear current turn-off.

6.2 Processing and interpretation of MT data

Time-series data downloaded from the MTU-5A unit were viewed using the Synchro Time Series View, running in a Windows environment. The program also allows viewing and printing of graphical representations of the raw time-series data (Figure 12), power spectral analysis of the data and coherence between pairs of orthogonal channels. Time series processing is done by SSMT2000, a program developed by Phoenix Geophysics, Canada.

Fourier transforms were produced from the raw time-series data. Reprocessing of Fourier coefficients from each station was then done using data from the remote reference station to filter out noisy data.

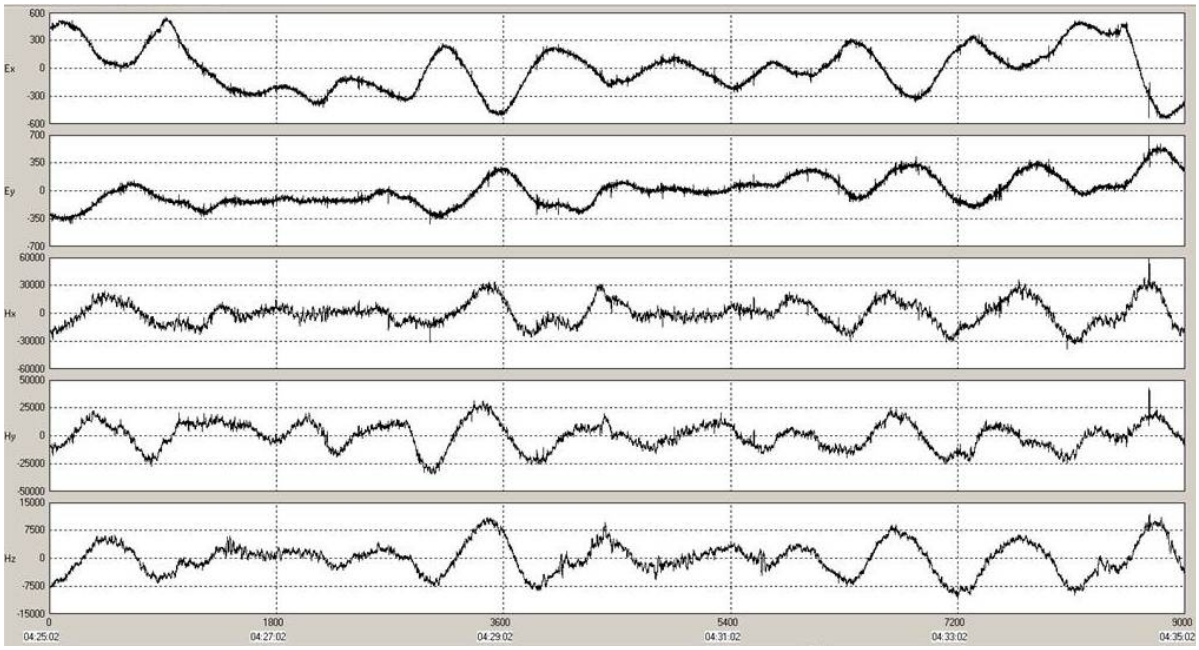

FIGURE 12: Time series recording of 10 minutes at a 5-channel MT site

The cross powers were stored as MTH and MTL files which can be displayed graphically using the MTeditor program. This program is also used to export by converting the cross powers (MPK files) into both PLT files (plotting format) and industry-standard EDI format for further interpretation with geophysical software. The TEMTD program was then used to invert the MT soundings (EDI files) jointly with the TEM soundings collected from the same site. The joint inversion curves are shown in Appendix II.

6.2.1 Robust processing parameters

The SSMT2000 offers two schemes for initial processing that attempt to filter out noise-affected data. These are controlled by robust processing parameters, coherency and rho variance. The process reduces the size of the error bars and smoothes the curves in plots of apparent resistivity (Figure 13). Coherency refers to eight processing schemes that compare measured site data with remote reference site data, and processes only the data that are coherent. Cultural noise at the sounding site but not at the reference site is thus reduced.

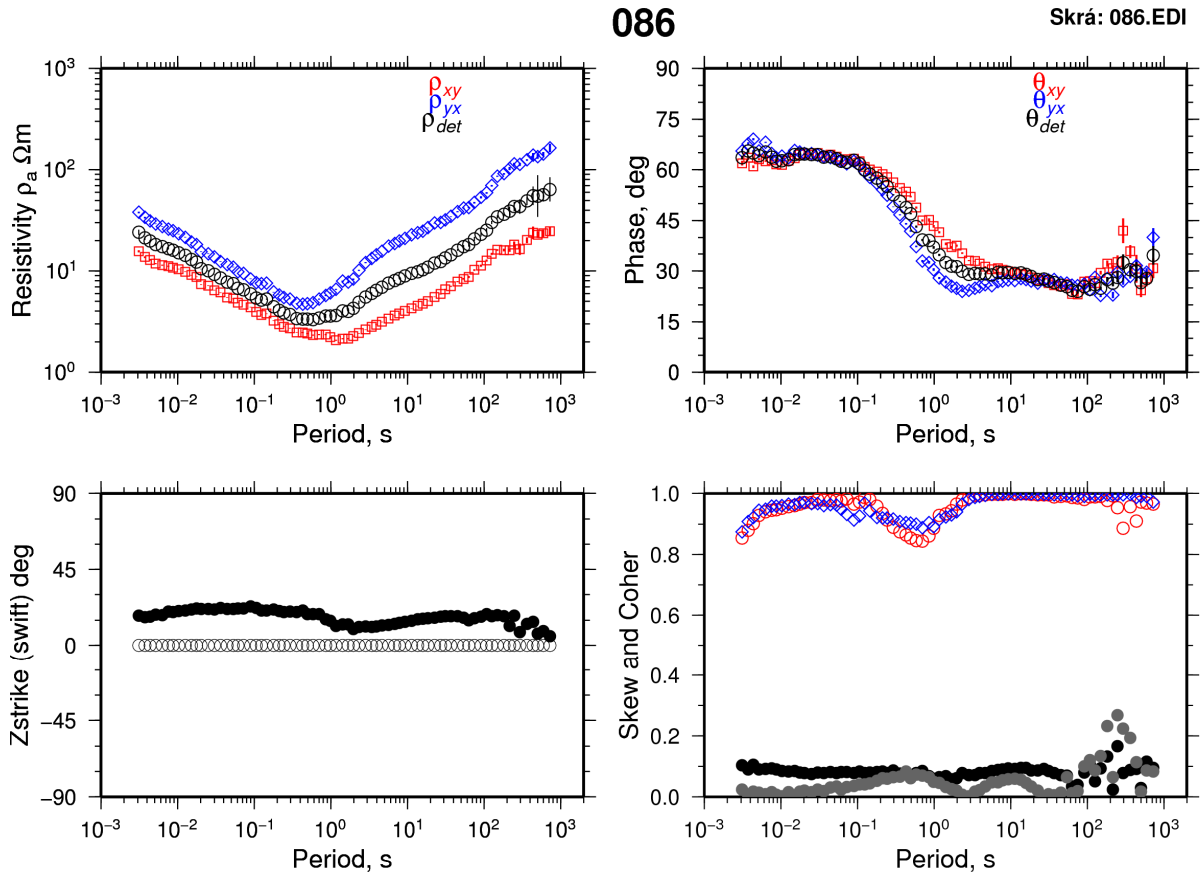

FIGURE 13: A typical result of MT data processing

Resistivity variance (rho variance) is a second stage of coherency processing that compares the telluric and magnetic results from the first stage, and selects data where these results are coherent. Robust parameter (PRM) files are unique to each site and, therefore, a single set of parameters cannot be used to process time series from another site. Data reduction involves applying some rule for out layer rejection, using estimation and testing procedures on the remainder.

6.3 The TEMTD program

The apparent resistivity curves for any resistivity soundings can be calculated for given layered earth models (Tugume, 1995). This means that one can determine the response that would be measured if the earth had a given layered structure; this is what is referred to as a solution to the forward problem. Therefore, interpretation of any measured resistivity data in terms of layered earth models can be done in principle by forward modelling. This involves guessing a layered structure and comparing the calculated response of the model to the measured data. By visual inspection of the differences between the measured and calculated response model, a new model is formulated.

1-D (layered earth) interpretation of resistivity data is nowadays done by inversion programs. An inversion program consists of a forward algorithm and an inversion algorithm (Árnason, 1989). The inversion algorithm is a procedure that calculates, from the differences between the calculated response of a given model and the measured data, adjustments to be done to the model parameters such that a better agreement is reached. This is applied iteratively until the difference in the calculated and measured responses cannot further be reduced.

In inversion of MT data, the forward algorithm is the standard complex impedance 1-D recursion algorithm described in Section 4.2 (Equation 35), while in the case of TEM the forward algorithm is as described in Section 4.1 (Árnason, 2006). The inversion algorithm used in the program is the Levenberg-Marquardt nonlinear least-squares inversion (Árnason, 1989). The misfit function is the root-mean square (RMS) difference between measured and calculated values (chisq), weighted by the standard deviation of the measured values. The program offers the possibility of keeping models smooth, both with respect to resistivity variations between layers (logarithm of conductivities) and layer thickness (logarithm of ratio of depth to top and bottom of the layers). The damping can be done both on first derivatives which counteracts sharp steps in the model, and on the second derivatives which counteracts oscillations in the model values. The actual function that is minimised is, therefore, not just the weighted RMS misfit, chisq, but the potential:

$$Pot = chisq + \alpha \times DS1 + \beta \times DS2 + \gamma \times DD1 + \delta \times DD2 \quad (37)$$

where DS1 and DS2 are the first and second order derivatives of log conductivities in the layered model, and DD1 and DD2 are the first and second order derivatives of the logarithms of the ratios of layer depths. The coefficients α, β, γ and δ are the relative contributions of the different damping terms. TEMTD can also perform Occam inversion (minimum structure), where the layer thicknesses are kept fixed, equally spaced on a log scale, and the conductivity distribution is forced to be smooth by adjusting α and β values in Equation 37. In Occam inversion the number of layers is normally between 20 and 40.

7. RESULTS FROM 1-D INVERSION

The output files (layered resistivity models), obtained from Occam inversion of TEM resistivity and joint inversion of TEM and MT soundings using a TEMTD inversion program, were used to generate resistivity cross-sections to different depths. A program TEMCROSS, developed and written by Dr. Hjálmar Eysteinsson (1998), was utilized to achieve this. The program runs on the basis of the GMT (generic mapping tools) program package to generate the output postscript files.

7.1 TEM resistivity cross-section

Resistivity cross-section KRY9

The TEM resistivity cross-section generated from the 1-D layered inversion of TEM soundings is shown in Figure 14. Two 700 m deep drill holes, KR-05 and KR-06, which are close to the profile,

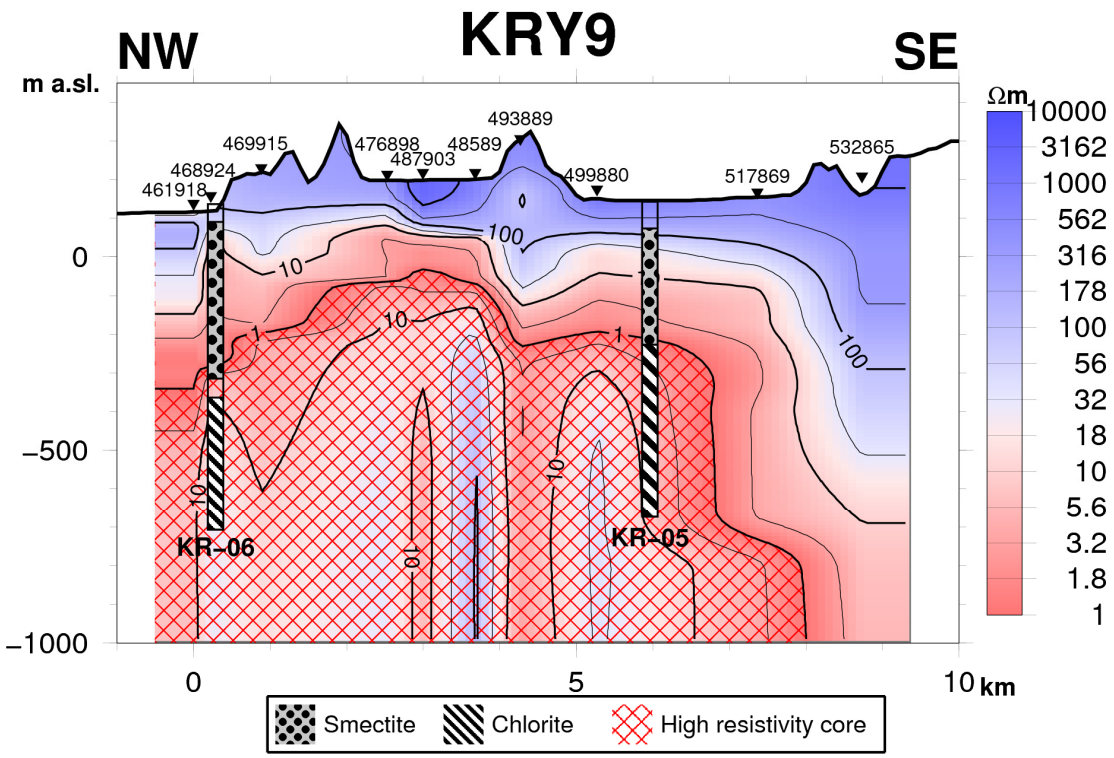

FIGURE 14: TEM resistivity cross-section KRY9 down to 1000 m b.s.l.

have been projected on to the cross-section. The resistivity cross-section runs in a SE-NW direction, and lies between Northings (7085-7093) and Eastings (0445-0454) in UTM coordinates (see Figure 11). A high-resistivity layer with resistivity >50 Ωm is dominant throughout the uppermost 200 m, and extends down to 500 m b.s.l. at the southeast end of the profile, below TEM sounding 532865. This high resistivity observed close to the surface is associated with fresh basaltic lavas and unaltered rocks. Below it a low-resistivity layer is seen with resistivity in the range of 1-10 Ωm. This layer is associated with the high-temperature geothermal system, showing the low-resistivity cap that outlines the high-temperature geothermal system. Below this layer, a highly resistive body is observed, which is also typical for the central part of high-temperature geothermal systems in Iceland. The data from the two drill holes on the cross-section clearly correlate with the resistivity distribution. They show conductive (alteration) minerals, with smectite and zeolites extending down to the top of the resistive core, where more resistive alteration minerals as chlorite, being seen at deeper levels.

7.2 MT resistivity cross-sections

Two resistivity cross-sections are shown in Figures 15 and 16 based on the results of the jointly inverted TEM and MT soundings performed along profile KRY9. Figure 15 shows the resistivity distribution down to 1000 m b.s.l., similar to Figure 14, while Figure 16 shows the resistivity distribution down to 5000 m b.s.l. The shallow drill holes, KR-05 and KR-06, are also projected and shown on the cross-section in Figure 15. The two cross-sections, show clearly the low-resistivity formation of <10 Ωm, extending approximately from 50-100 m a.s.l. down to approx.500 m b.s.l. The resistivity structure (low-resistivity layer around a resistive core) defined in the MT cross-sections is analogous to a traditional the traditional resistivity distribution seen in high-temperature geothermal fields, as mentioned above. The cross-section in Figure 15 shows a close similarity with the TEM cross-section in Figure 14, in the uppermost kilometre. At deeper levels, below 1000 m b.s.l. no significant change in the resistivity distribution was observed, with the high-resistivity layer, with resistivity >50 Ωm, extending down to 5000 m b.s.l. As discussed above, the secondary alteration distribution in the drill holes correlates well with the resistivity distribution.

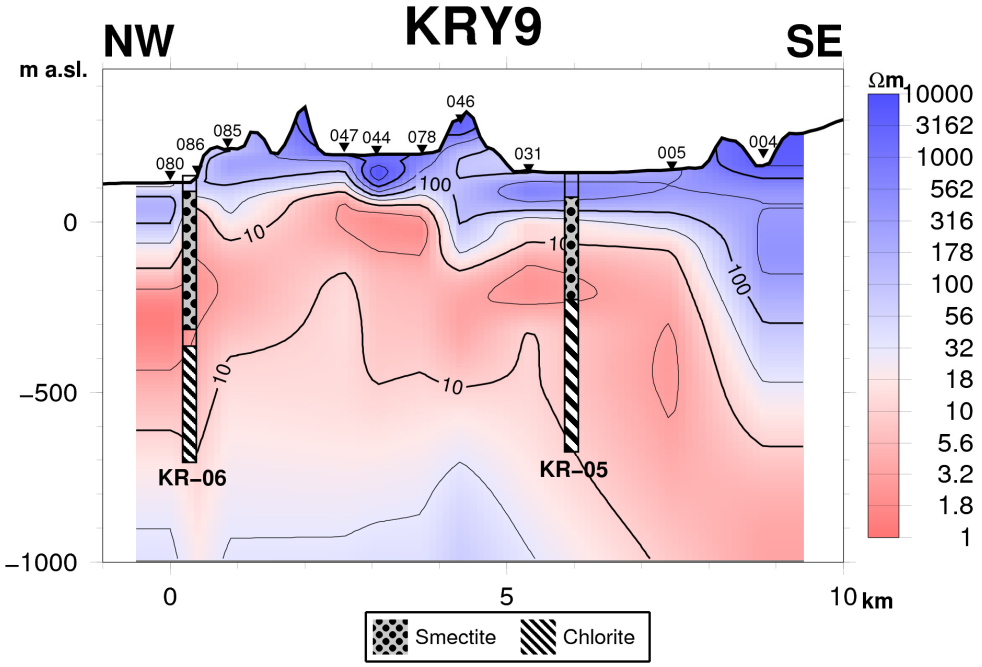

FIGURE 15: MT resistivity cross-section KRY9 down to 1000 m b.s.l.

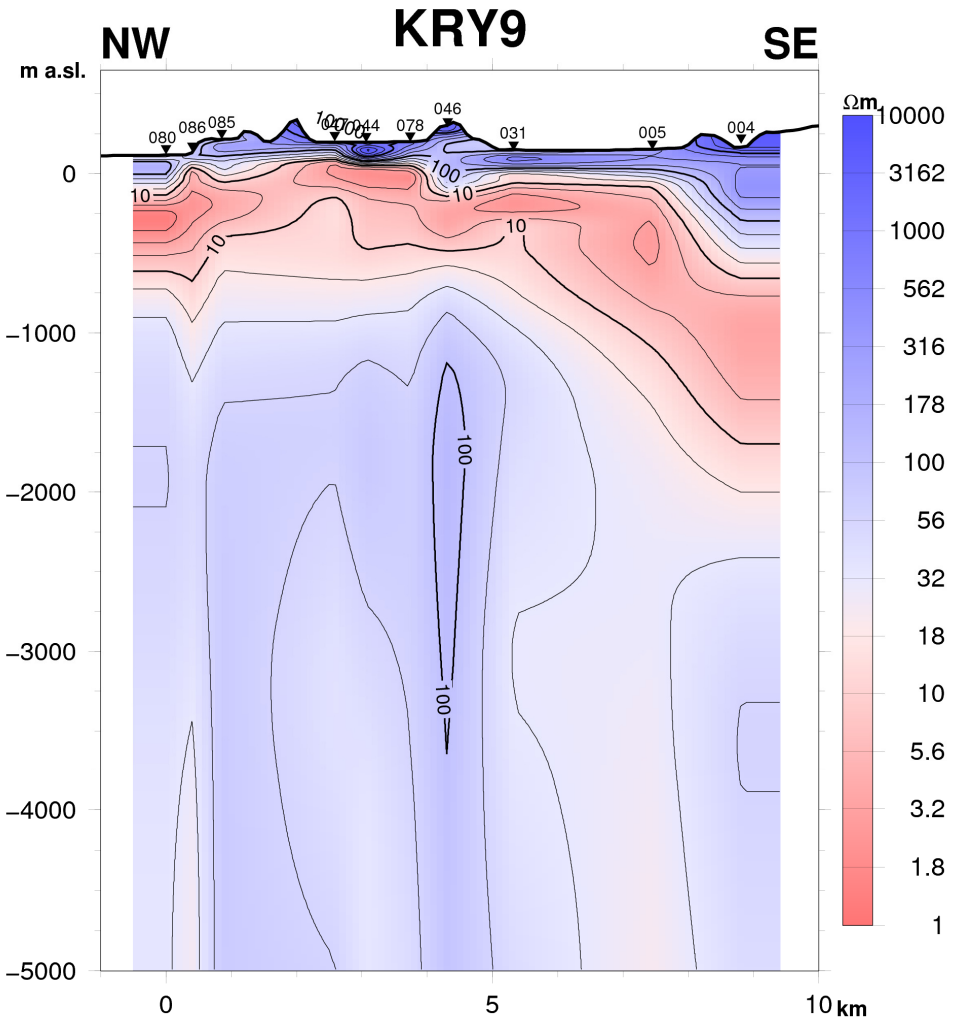

FIGURE 16: MT resistivity cross-section KRY9 down to 5000 m b.s.l.

8. GEOTHERMAL INTERPRETATION

The characteristics in the resistivity structure of high-temperature geothermal fields in Iceland are a resistive surface, below which a low-resistivity cap is found underlain by a high-resistivity core. The low-resistivity is defined by values in the range of 1-10 Ωm in fresh water systems. The high-resistivity core has resistivity values of at least an order of magnitude higher than that of the low-resistivity cap. The outer margin of the low-resistivity cap delineates the high-temperature system.

Interpretation of resistivity data and the models obtained have revealed that the resistivity structure of high-temperature geothermal systems in Iceland is controlled by the secondary alteration status of the rocks. The comparison between mineral alteration and temperature in most geothermal systems indicates a consistent correlation. If the mineral alteration is in equilibrium with temperature, the cold resistive rocks with temperatures below 50°C are fresh and unaltered. Between temperatures of 50 and 200°C, the alteration increases gradually with the formation of the dominant alteration minerals for this temperature interval, smectite and zeolites. At deeper levels, at temperatures in the range of 200-240°C, the zeolite disappears and smectite gradually transforms into chlorite. In the range of 240-250°C, the resistive chlorite becomes the dominant alteration mineral. Above 250°C, epidote and other resistive high-temperature minerals are abundant.

The comparison between the resistivity structure and secondary alteration mineralogy generally shows highly resistive rocks close to the surface, reflecting fresh unaltered rocks. The low-resistivity cap below is found to coincide with the smectite-zeolite zone, as these minerals are very conductive. At still deeper levels the appearance of the resistive core coincides with the mixed layer clay and chlorite zone taking over in the alteration mineralogy, changing to the resistive chlorite and epidote at deeper levels. The resistivity cross-section presented in the previous chapter show similar structure as described above, and this can be interpreted in terms of geothermal activity, with the low-resistivity cap around a high-resistivity core, appearing in the central part of the profile.

9. SUMMARY AND CONCLUSIONS

An extensive electromagnetic resistivity survey has been carried out in the Krýsuvík area during the last decade, giving better resolution of the resistivity distribution in the area compared to older surveys with Schlumberger soundings carried in the seventies and eighties. A total of 10 TEM resistivity soundings and 10 new MT soundings were jointly interpreted as a part of this project. Integrated data interpretation was carried out using the 1-D layered inversion program, TEMTD. The interpreted data are presented in the form of resistivity cross-sections, data curves and layered models. Eight shallow drill holes have been drilled in Krýsuvík area, of which two are located close to the profile. These were projected on to the cross-section to compare the resistivity distribution with the alteration mineralogy in the wells.

Although the soundings interpreted are limited to a single profile, the results obtained from the interpretation reveal a similar resistivity distribution of the basaltic rocks within the uppermost kilometre, as seen in other cross-sections in the area. The resistivity is quite high in the uppermost 100-300 m, falling in the range of 100-6000 Ωm. This high-resistivity close to the surface is correlated with fresh basalts and unaltered rocks where hydrothermal alteration is minimal. Below that, the resistivity is low (the low-resistivity cap); with the resistivity obviously influenced by conductive geothermal alteration, indicated by resistivity values in the range of 1-10 Ωm. Higher resistivity is seen again at deeper levels, at a depth of 500-1000 m, with the resistivity increasing by an order of magnitude, thus defining the resistive core of the high-temperature geothermal system.

Based on the results obtained from the integrated interpretation of resistivity data, the resistivity structure in Krýsuvík area can be summarised as follows:

- A low-resistivity cap, underlain by a high-resistivity core exists beneath Krýsuvík geothermal area. The low resistivity coincides with the smectite-zeolite zone, characterized by conductive alterations minerals.
- The resistive core reaches highest to an elevation of approximately 150 m b.s.l., which means that the top of the high-resistivity core is about 350-400 m deep from the surface of the study area. The resistive layer coincides with the chlorite-epidote zone.
- There is a fairly good correlation between the measured resistivity and hydrothermal alteration in the drill holes.
- The temperature in the high-resistivity core is expected to exceed 230-240°C, provided there is equilibrium between thermal alteration of the rocks and the present temperature in the reservoir.
- It is probable that this resistivity structure extends along the NE-SW fissure swarm.

ACKNOWLEDGEMENTS

It is my pleasure to acknowledge the Government of Iceland and the United Nations University for accepting my application and for their sponsorship. My special thanks go to UNU-GTP director Dr. Ingvar Birgir Fridleifsson and the deputy director Mr. Lúdvík S. Georgsson for confirming my coming to Iceland, to Ms. Thórhildur Ísberg, Ms. Dorthe H. Holm and Mr. Markús A.G. Wilde for all their guidance and assistance rendered during my stay in Iceland. I am indebted to all ÍSOR geophysical staff, especially my advisor Mr. Arnar Már Vilhjálmsson, assisted by Dr. Hjálmar Eysteinsson and Mr. Gylfi Páll Hersir for all their valuable input and critical comments, especially during data processing and interpretation. I greatly appreciate Mr. Knútur Árnason for his critical review of the manuscript. I further thank ÍSOR for availing data and the software used. All the lecturers are greatly acknowledged for their valuable time spent during preparation and presenting of the lecture materials and arranging field demonstrations and excursions.

I am grateful to my employer, the Ministry of Energy and Mineral Development through the Department of Geological Survey and Mines for granting me a study leave. I would like to express my sincere thanks to my relatives, particularly my wife, Lydia Nayiga and our daughter Lostina M. Namuwaya for enduring my absence from home. My success in this study was possible with all your support, encouragement and prayers. I dedicate this work to my lovely daughter, Lostina.

REFERENCES

Archie, G.E., 1942: The electrical resistivity log as an aid in determining some reservoir characteristics. *Tran. AIME, 146,* 54-67.

Ármannsson, H., Thórhallsson, S., and Ragnarsson, Á., 1994: *Krýsuvík-Trölladyngja. Potential steam production and transmission to energy park, Straumsvík.* Orkustofnun, Reykjavík, report OS-94012/JHS-07B, 17 pp.

Árnason, K., 1989: *Central loop transient electromagnetic sounding over a horizontally layered earth*. Orkustofnun, Reykjavík, report OS-89032/JHD-06, 128 pp.

Árnason, K., 2006: *TEMTD (A program for 1-D inversion of central-loop TEM and MT data)*. ÍSOR – Iceland GeoSurvey, Reykjavík, short manual, 16 pp.

Árnason, K., and Flóvenz, Ó.G., 1992: Evaluation of physical methods in geothermal exploration of rifted volcanic crust. *Geoth. Res Council, Trans., 16,* 207-214.

Árnason, K., Karlsdóttir, R., Eysteinsson, H., Flóvenz, Ó.G., and Gudlaugsson, S.Th., 2000: The

resistivity structure of high-temperature geothermal systems in Iceland. *Proceedings of the World Geothermal Congress 2000*, *Kyushu-Tohoku, Japan,* 923-928.

Árnason, K., Vilhjálmsson, A.M., and Björnsdóttir, Th., 2009: A study of the Krafla volcano using gravity, micro earthquake and MT data. In: Georgsson, L.S., Mariita, N., and Simiyu, S.M. (eds.), *Short Course IV on Exploration for Geothermal Resources.* UNU-GTP, KenGen, GDC, CD SC-10, 14 pp.

Arnórsson, S., Björnsson, A., Gíslason, G., and Gudmundsson, G., 1975: Systematic exploration of the Krísuvík high-temperature area, Reykjanes Peninsula, Iceland. *Proceedings of the 2nd U.N. Symposium on the Development and Use of Geothermal Resources, San Francisco, 1,* 853-864.

Clifton A., 2007: *Tectonic – magmatic interaction at an oblique rift zone*. Nordic Volcanological Institute, report, website: *www.norvol.hi.is/~amy/ReykjanesFieldTrip.pdf*, 9 pp.

Dakhnov, V.N., 1962: Geophysical well logging. *Q. Colorado Sch. Mines, 57-2*, 445 pp.

Eysteinsson, H., 1998: *TEMRESD, TEMMAP and TEMCROSS plotting programs.* ÍSOR – Iceland GeoSurvey, unpublished programs and manuals.

Eysteinsson, H., Árnason, K. and Flóvenz, Ó.G., 1993: Resistivity methods in geothermal prospecting in Iceland. *Surveys in Geophysics, 15,* 263-275.

Flóvenz, Ó.G., Fridleifsson, G.Ó., Johnsen, G.V., Kristmannsdóttir, H., Georgsson, L.S., Einarsson, S., Thórhallsson, S., and Jónsson, S.L., 1986: *Vatnsleysa-Trölladyngja, freshwater and geothermal investigation. 3 Geothermal exploration*. Orkustofnun, Reykjavík, report OS-86032/JHD-10 B, 39-92.

Flóvenz, Ó.G., Spangenberg, E., Kulenkampff, J., Árnason, K., Karlsdóttir, R., and Huenges, E., 2005: The role of electrical interface conduction in geothermal exploration. *Proceedings of World Geothermal Congress 2005, Antalya, Turkey*, CD, 9 pp.

Hermance, J.F., 1973: Processing of magnetotelluric data. Physics of the Earth and Planetary Interiors, 7, 349-364.

Hermance, J.F., 1995: Electrical conductivity models of the crust and mantle. In: Ahrens, T. (ed.), *Handbook of physical constants.* AGU, 190-205.

Hersir, G.P., and Björnsson, A., 1991: *Geophysical exploration for geothermal resources. Principles and applications*. UNU-GTP, Iceland, report 15, 94 pp.

Hersir, G.P., Rosenkjær, G.K., Vilhjálmsson, A.M., Eysteinsson, H., and Karlsdóttir, R., 2009: *The Krýsuvík geothermal field. Resistivity soundings 2007 and 2008*. ÍSOR - Iceland GeoSurvey, Reykjavík, report (in Icelandic), in prep.

Imsland, P., 1973: *The geology of Sveifluháls.* University of Iceland, B.Sc. thesis (in Icelandic), 87 pp.

Jónsson, J., 1978: *A geological map of the Reykjanes Peninsula*. Orkustofnun, Reykjavík, report OS/JHD 7831 (in Icelandic), 333 pp and maps.

Kearey, P., and Brooks, M., 1994: *An introduction to geophysical exploration* (2nd edition). Blackwell Scientific Publ., London, 236 pp.

Keller, G.V., and Frischknecht, F.C., 1966: *Electrical methods in geophysical prospecting.* Pergamon Press Ltd., Oxford, 527 pp.

Kurt, I. S., Anders, V.C., and Esben, A., 2006: *The transient electromagnetic method (TEM).* Burval, website: burval.org/final/pdf/065-076.pdf, 12 pp.

Morris, F.H., and Becker, A., 2001: *Berkeley course in applied geophysics*. University of California, Berkeley, CA, lecture notes, unpublished.

Pálmason, G., 1971: *Crustal structure of Iceland from explosion seismology.* Soc. Scient. Islandica, XL, 187 pp.

Phoenix Geophysics, 2003: *V5 System 2000MTU/MTU-A user guide.* Phoenix Geophysics, Ltd., Toronto.

Rink, M., and Shopper, J.R. 1976: Pore structure and physical properties of porous sedimentary rocks. *Pure Appl. Geophys., 114,* 273-284.

Sternberg, B.K., Washburn, J.C., and Pellerin, L., 1988: Correction for the static shift in magnetotellurics using transient electromagnetic soundings. *Geophysics, 53-11,* 1459-1468.

Tugume, M.F., 1995: One-dimensional interpretation of Schlumberger and TEM resistivity data with examples from Torfajökull, S-Iceland. Report 14 in: *Geothermal Training in Iceland 1995.* UNU-GTP, Iceland, 349-382.

Volpi, G., Manzella, A., and Fiordelisi, A., 2003: Investigation of geothermal structures by magnetotellurics (MT): An example from the Mt. Amiata area, Italy. *Geothermics, 32,* 131-145.

Vozoff, K., 1990: Magnetotellurics: Principles and practices. *Proc. Indian Acad. Sci.,Earth Planetary Science, 99-4*, 441-471.

Ward, S.H., and Wannamaker, P.E., 1983: *The MT/AMT electromagnetic method in geothermal exploration.* UNU-GTP, Iceland, report 5, 107 pp.

Zhdanov, M.S., and Keller, G.V., 1994: *The geoelectrical methods in geophysical exploration. Methods in geochemistry and geophysics, 31.* Elsevier Scientific Publ. Co., 884 pp.

APPENDIX I: 1-D modelling of TEM soundings using TEMTD

In each plot of the TEM resistivity soundings presented below, the red (dark) dotted curve represents the measured TEM data curve, the black curve represents the calculated TEM data, and the green (gray) line is the obtained 1-D layered model which best suits the data.

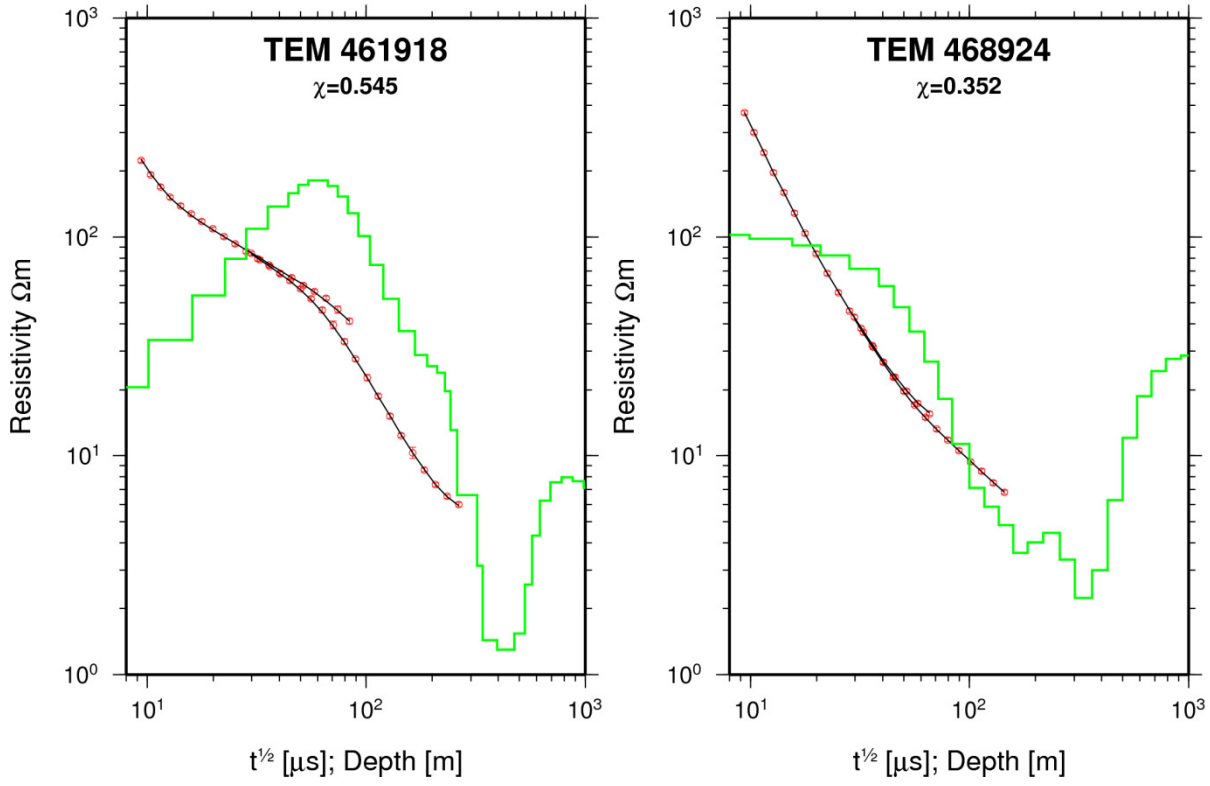

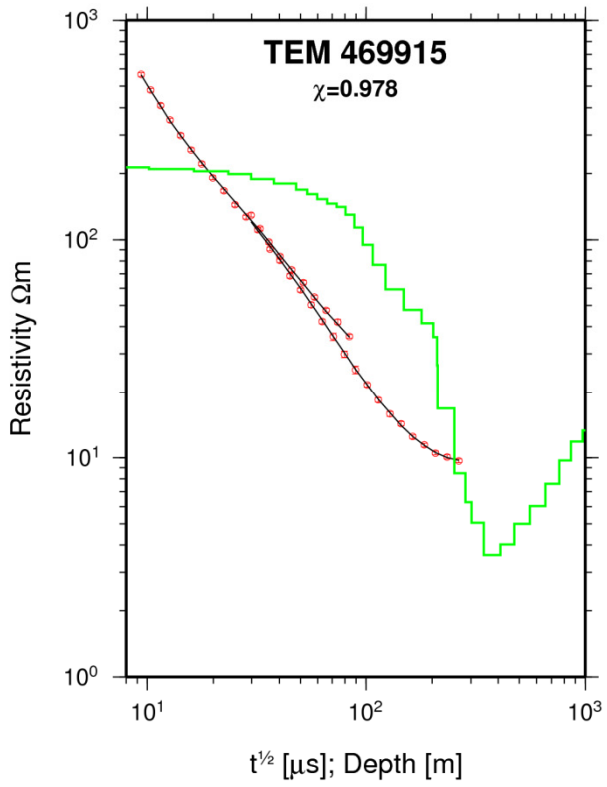
TEM 469915
χ=0.978
Resistivity Ωm
t½ [µs]; Depth [m]

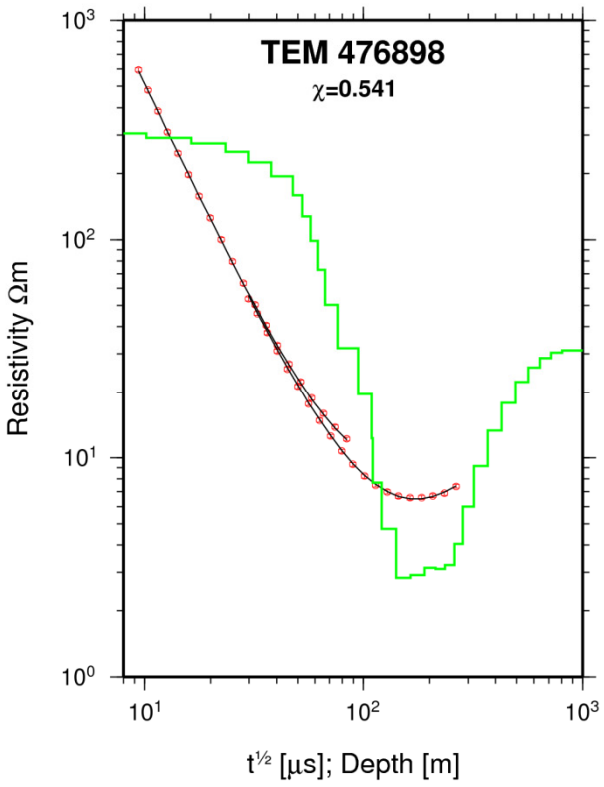
TEM 476898
χ=0.541
Resistivity Ωm
t½ [µs]; Depth [m]

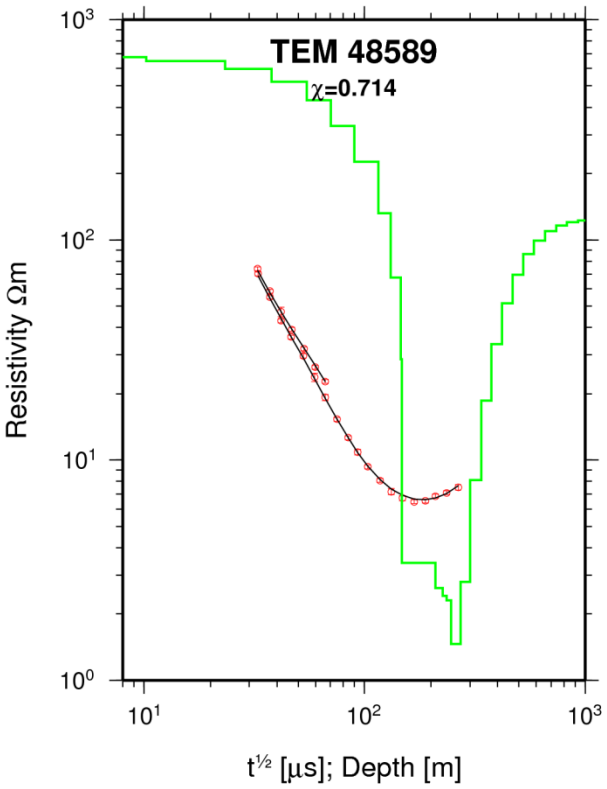
TEM 48589
χ=0.714
Resistivity Ωm
t½ [µs]; Depth [m]

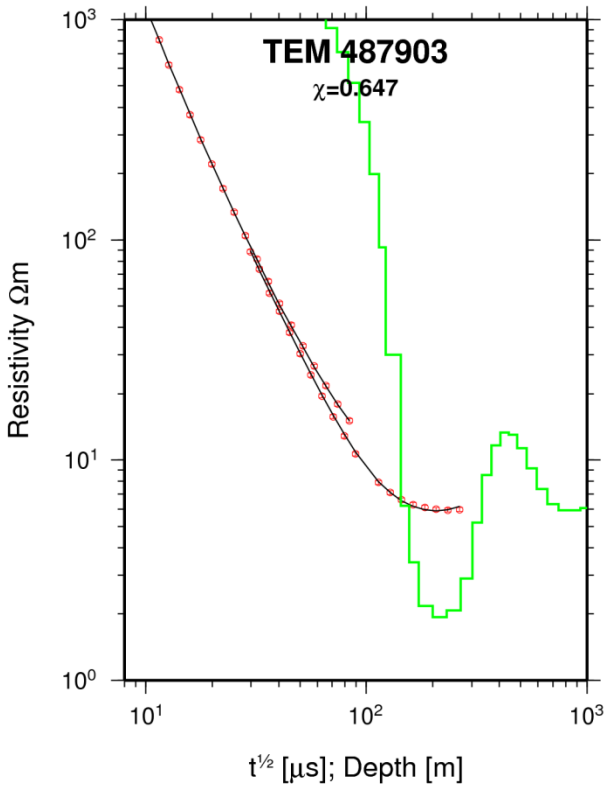
TEM 487903
χ=0.647
Resistivity Ωm
t½ [µs]; Depth [m]

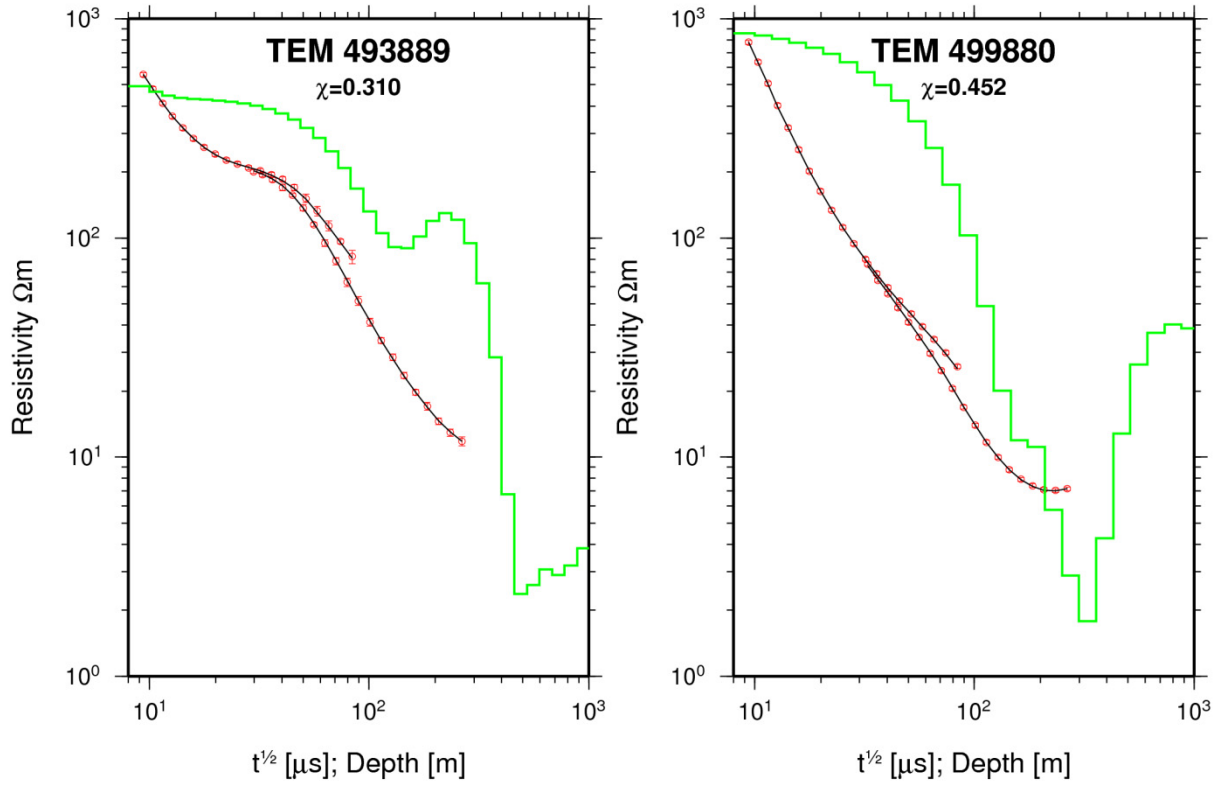
TEM 493889
χ=0.310
Resistivity Ωm
t½ [µs]; Depth [m]

TEM 499880
χ=0.452
Resistivity Ωm
t½ [µs]; Depth [m]

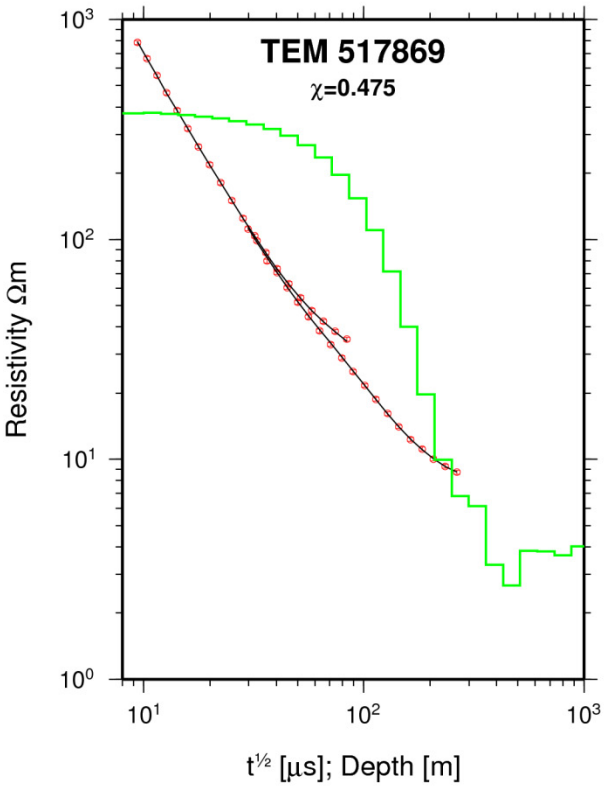
TEM 517869
χ=0.475
Resistivity Ωm
t½ [µs]; Depth [m]

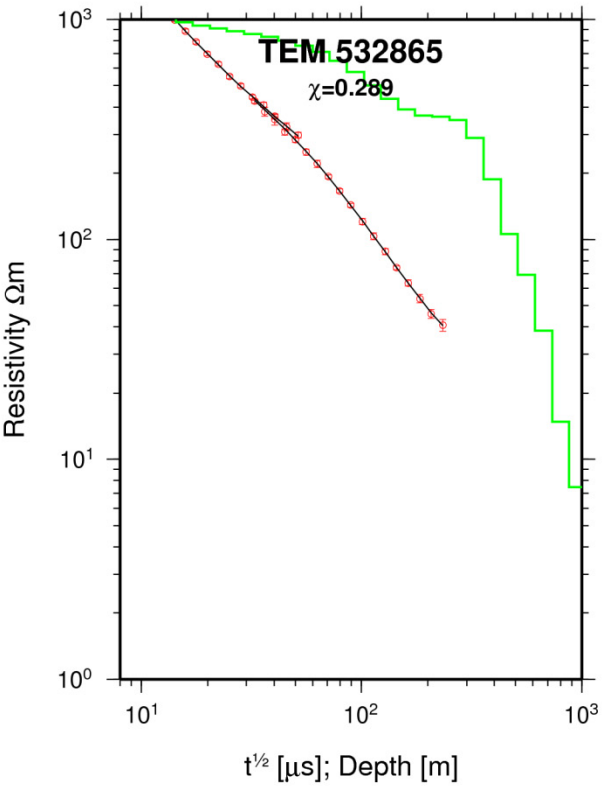
TEM 532865
χ=0.289
Resistivity Ωm
t½ [µs]; Depth [m]

APPENDIX II: Joint 1-D inversion models of MT and TEM soundings obtained using TEMTD

The red (dark) squares represent the measured TEM apparent resistivity, the blue (gray) squares are the apparent resistivity derived from the MT sounding data and the blue (gray) circles represent the phase. The solid lines through the plots show the response of the resistivity models shown on the right in each case.

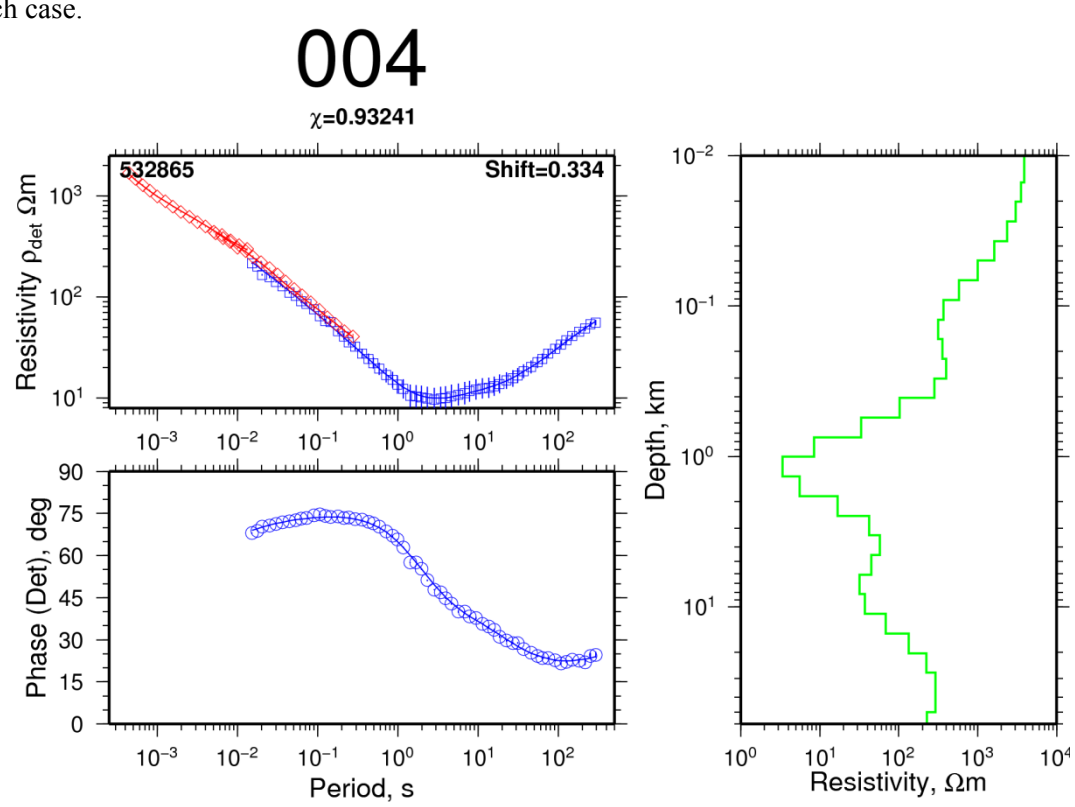

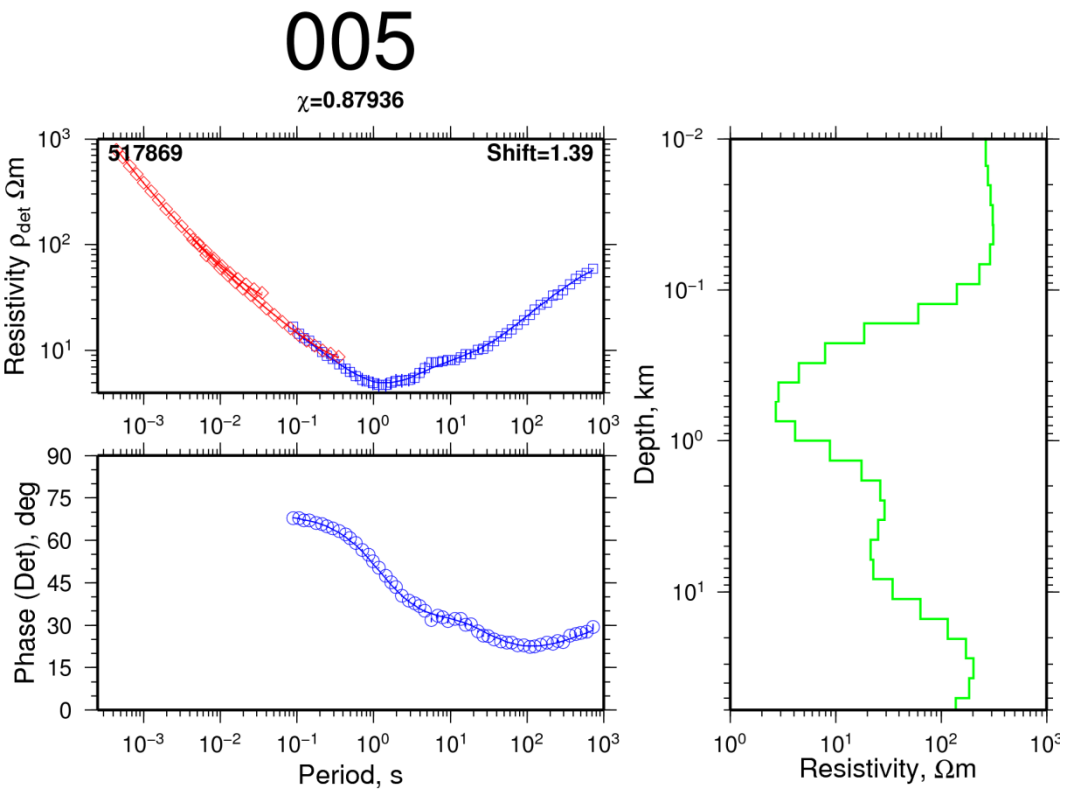

031

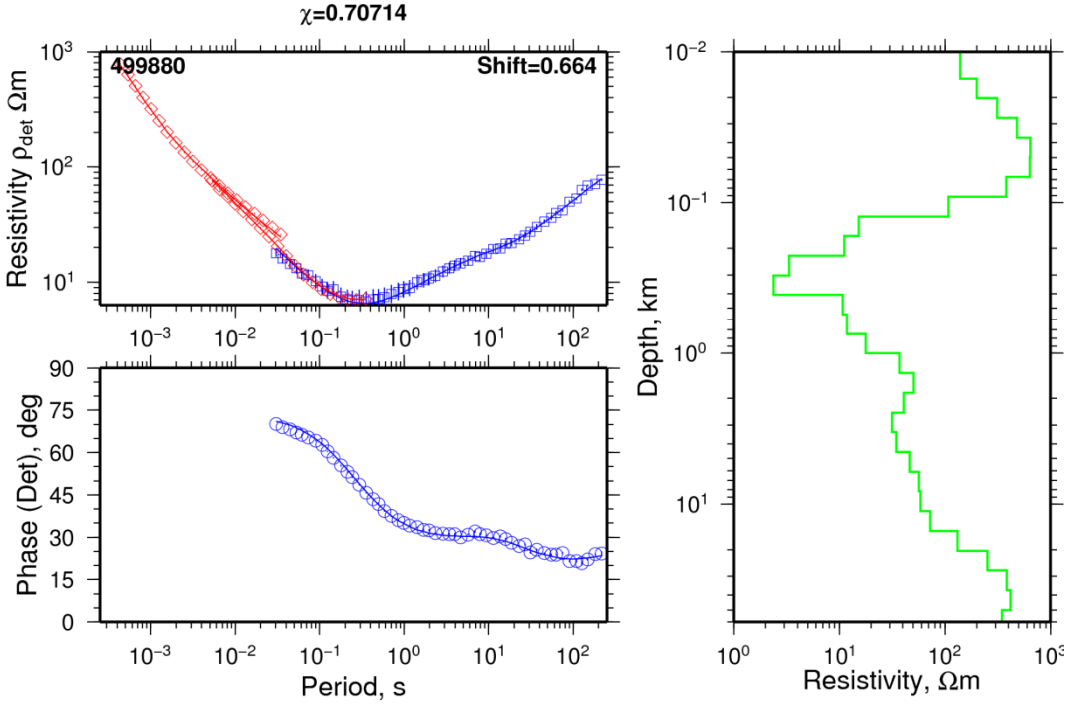
χ=0.70714
499880
Shift=0.664
Resistivity ρdet Ωm
Phase (Det), deg
Period, s
Depth, km
Resistivity, Ωm

044

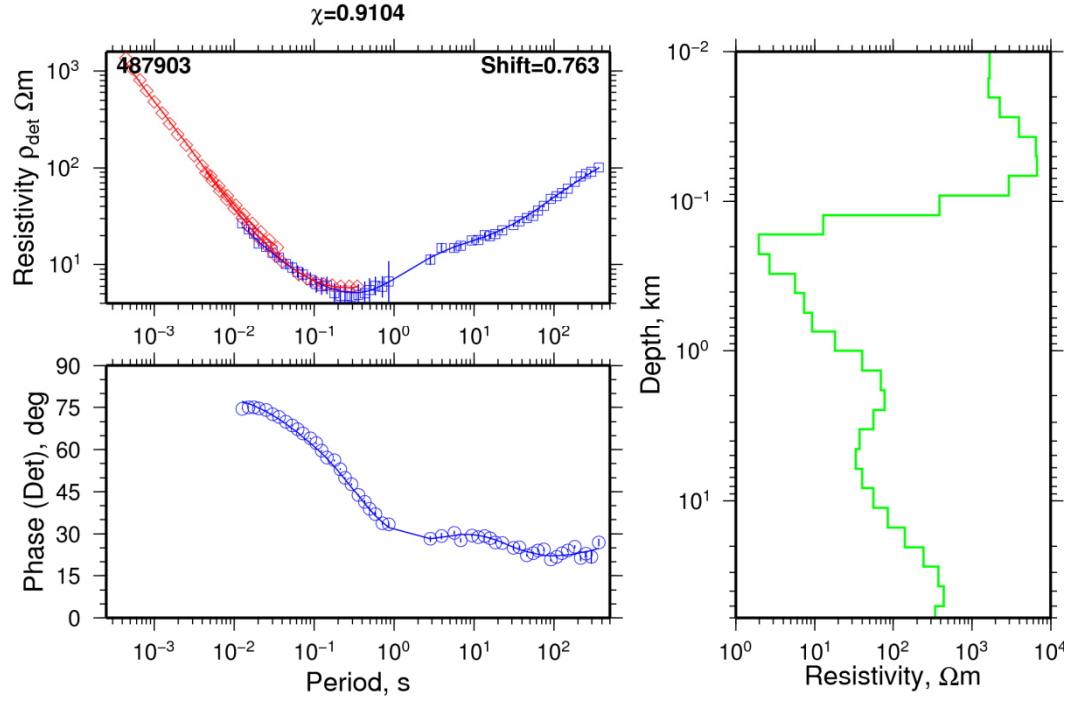
χ=0.9104
487903
Shift=0.763
Resistivity ρdet Ωm
Phase (Det), deg
Period, s
Depth, km
Resistivity, Ωm

046

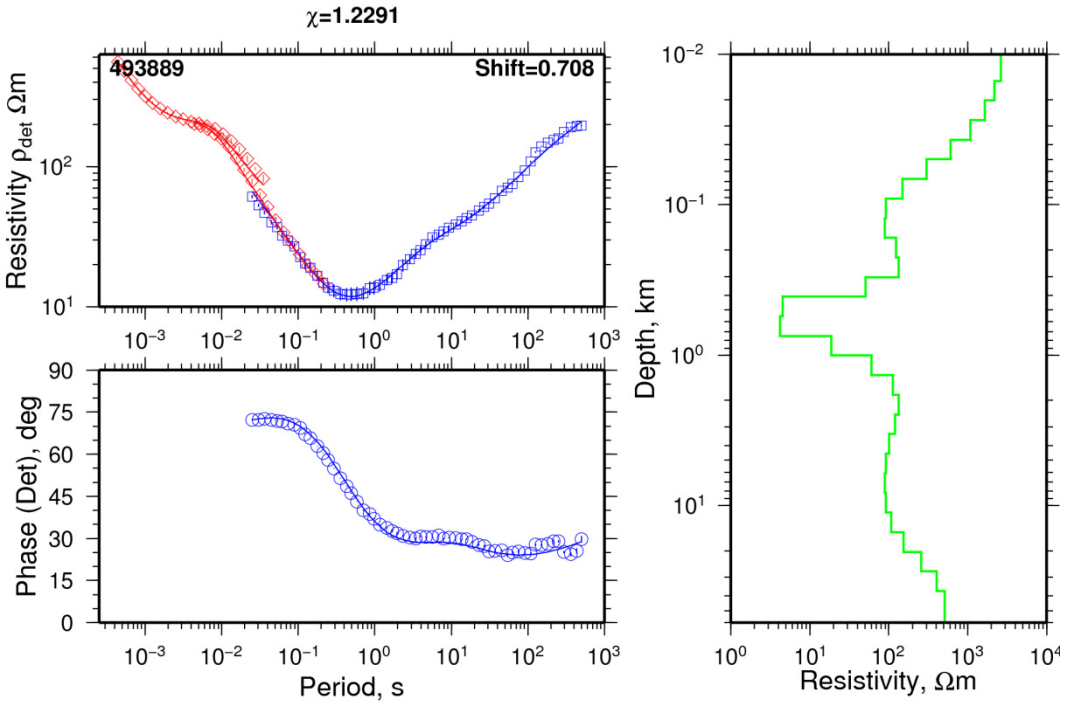
χ=1.2291
493889
Shift=0.708
Resistivity ρdet Ωm
Phase (Det), deg
Period, s
Depth, km
Resistivity, Ωm

047

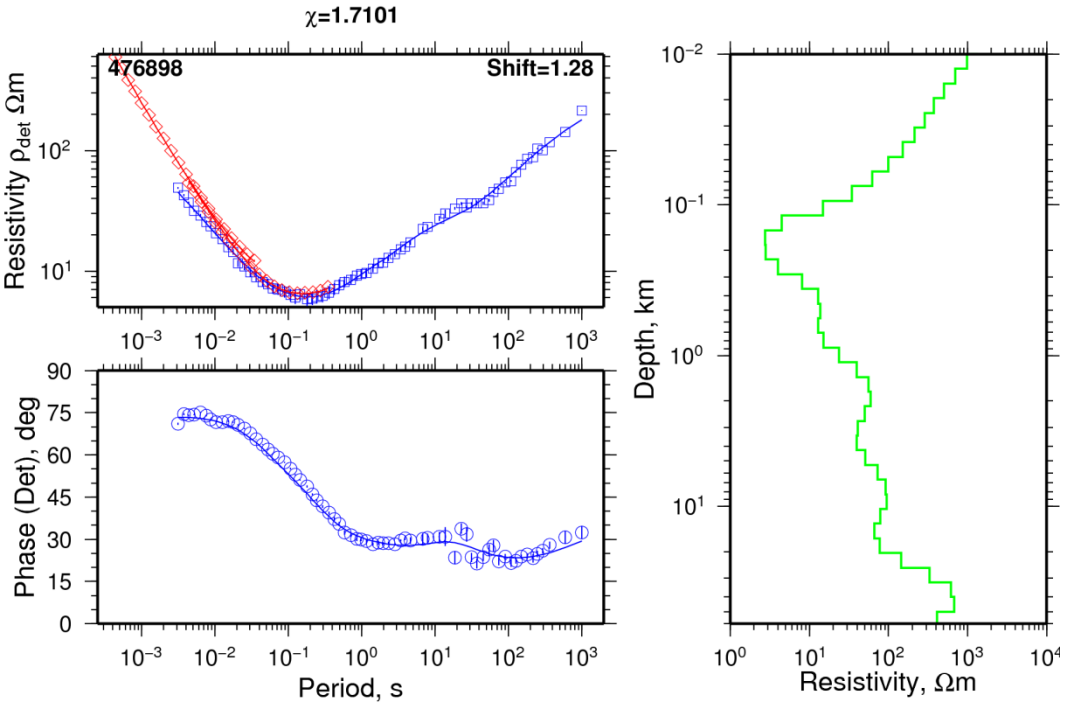
χ=1.7101
476898
Shift=1.28
Resistivity ρdet Ωm
Phase (Det), deg
Period, s
Depth, km
Resistivity, Ωm

078

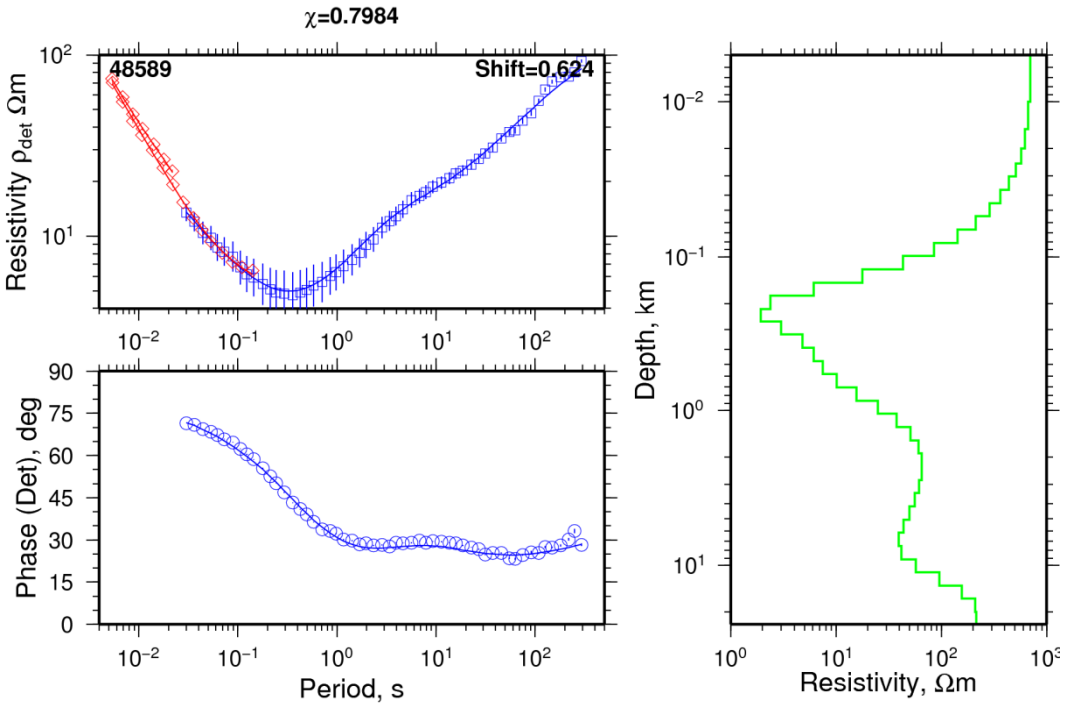
χ=0.7984
48589
Shift=0.624
Resistivity ρdet Ωm
Phase (Det), deg
Period, s
Depth, km
Resistivity, Ωm

080

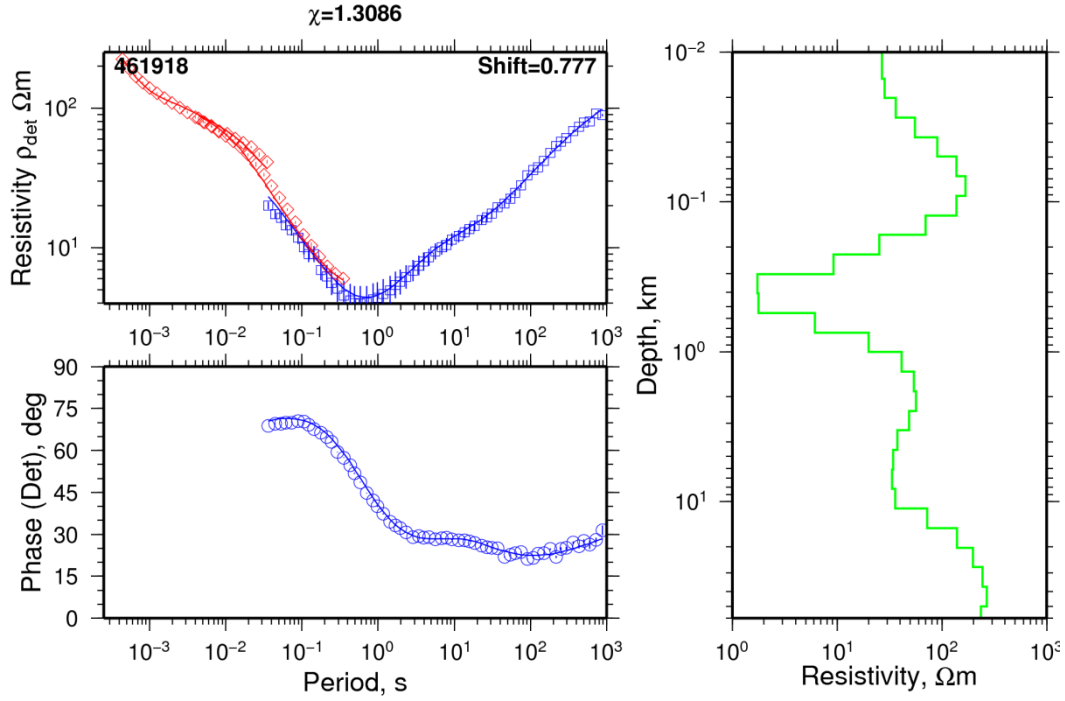
χ=1.3086
461918
Shift=0.777
Resistivity ρdet Ωm
Phase (Det), deg
Period, s
Depth, km
Resistivity, Ωm

085

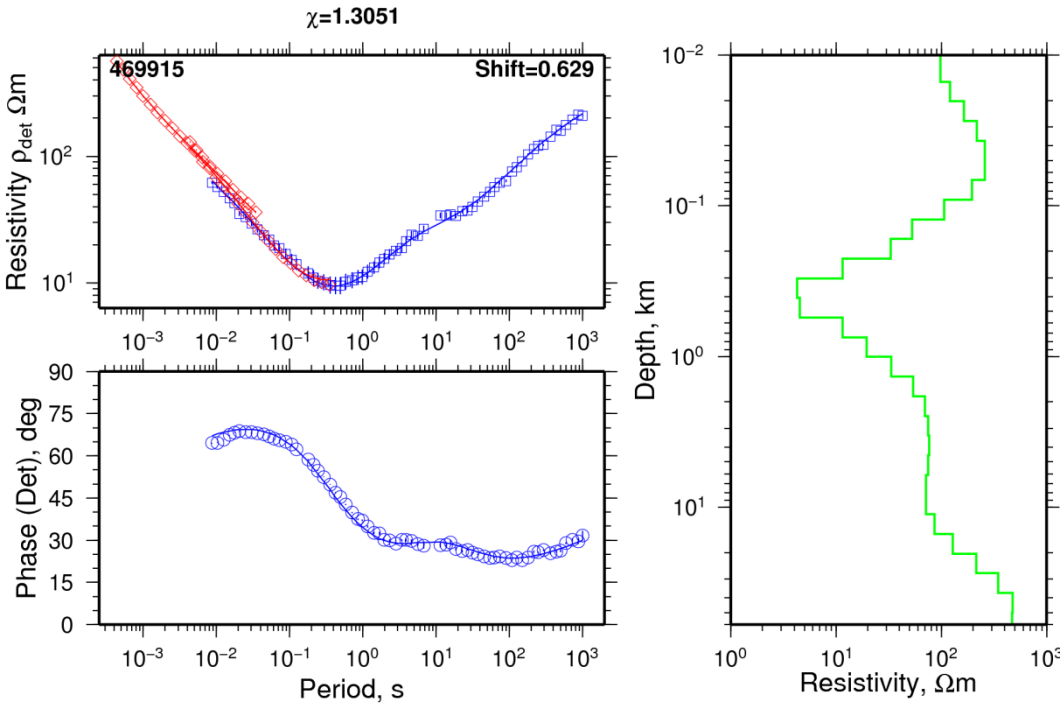
χ=1.3051
469915
Shift=0.629
Resistivity ρdet Ωm
Phase (Det), deg
Period, s
Depth, km
Resistivity, Ωm

086

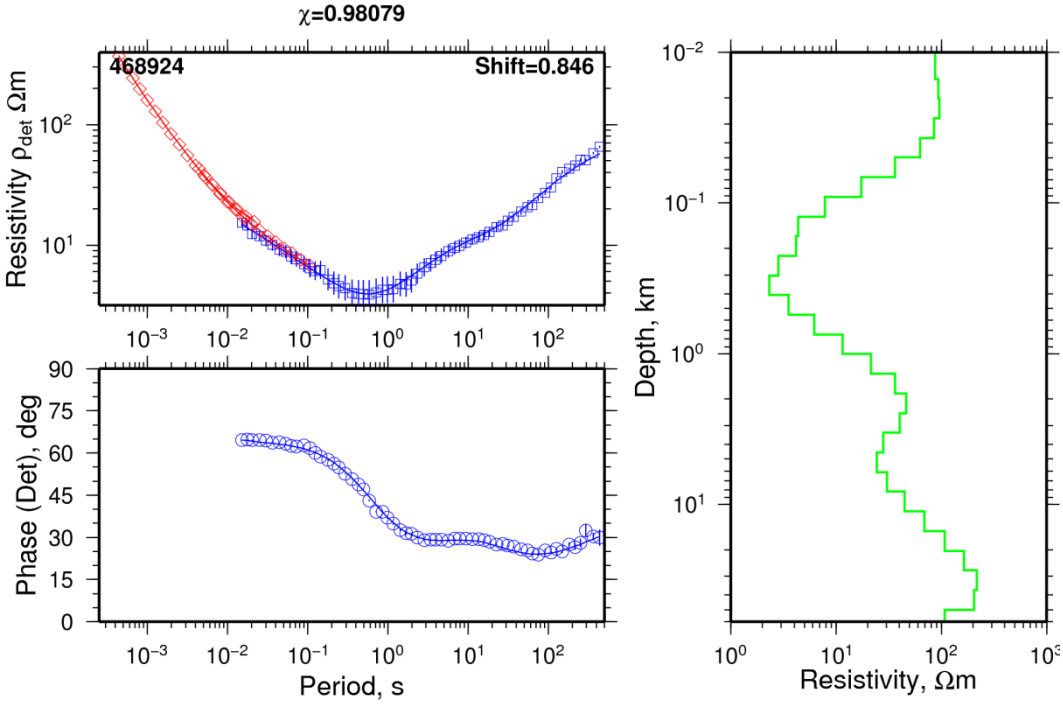
χ=0.98079
468924
Shift=0.846
Resistivity ρdet Ωm
Phase (Det), deg
Period, s
Depth, km
Resistivity, Ωm